STRUCTURAL CHEMISTRY

ISSN: 2053-2296
journals.iucr.org/c

Competition between chalcogen and halogen bonding assessed through isostructural species

Viraj De Silva, Pierre Le Magueres, Boris B. Averkiev and Christer B. Aakeröy

Acta Cryst. (2022). C**78**, 716–721

STRUCTURAL CHEMISTRY

ISSN 2053-2296

Competition between chalcogen and halogen bonding assessed through isostructural species

Viraj De Silva,[a] Pierre Le Magueres,[b] Boris B. Averkiev[a] and Christer B. Aakeröy[a]*

[a]Kansas State University, 213 CBC Building, Manhattan, Kansas 66506, USA, and [b]Rigaku Americas Corporation, 9009 New Trails Drive, The Woodlands, TX 77381, USA. *Correspondence e-mail: aakeroy@ksu.edu

Received 23 August 2022
Accepted 1 November 2022

Edited by L. Brammer, University of Sheffield, United Kingdom

Keywords: halogen bonding; chalcogen bonding; Hirshfeld surfaces; isostructural; molecular electrostatic potential; energy framework; interaction energies; crystal structure.

CCDC references: 2202927; 2202928; 2202931; 2202932

Supporting information: this article has supporting information at journals.iucr.org/c

The amino group of 2-amino-5-(4-halophenyl)-1,3,4-chalcogenadiazole has been replaced with bromo/iodo substituents to obtain a library of four compositionally related compounds. These are 2-iodo-5-(4-iodophenyl)-1,3,4-thiadiazole, $C_8H_4I_2N_2S$, 2-bromo-5-(4-bromophenyl)-1,3,4-selenadiazole, $C_8H_4Br_2N_2Se$, 2-bromo-5-(4-iodophenyl)-1,3,4-selenadiazole, $C_8H_4BrIN_2Se$, and 2-bromo-5-(4-iodophenyl)-1,3,4-thiadiazole, $C_8H_4BrIN_2S$. All were isostructural and contained bifurcated Ch···N (Ch is chalcogen) and $X\cdots X$ (X is halogen) interactions forming a zigzag packing motif. The noncovalent Ch···N interaction between the chalcogen-bond donor and the best-acceptor N atom appeared preferentially instead of a possible halogen bond to the same N atom. Hirshfeld surface analysis and energy framework calculations showed that, collectively, a bifurcated chalcogen bond was stronger than halogen bonding and this is more structurally influential in this system.

1. Introduction

1,3,4-Chalcogenadiazole moieties are often explored for their anti-inflammatory and anticancer properties (Genis *et al.*, 2009; Kumar *et al.*, 2008; Hu *et al.*, 2014). Their biological functions can be related to their molecular structures and unique abilities for forming a variety of structure-directing intermolecular interactions. In this context, it was shown recently that the balance between hydrogen, halogen, and chalcogen bonding can be altered by carrying out specific atom-for-atom substitution in 2-amino-1,3,4-chalcogenadiazole derivatives (De Silva *et al.*, 2021). One of the many issues that can prevent pharmaceutically active species from realizing their practical potential is a sub-optimal aqueous solubility. In order to better understand how molecular structure directly connects to specific physical properties of the bulk materials, it is therefore critically important to fully explore the structural landscape of this family of compounds.

In order to map out the potential competing nature of the halogen and chalcogen bonds, a diverse set of targets was synthesized, namely, 2-iodo-5-(4-iodophenyl)-1,3,4-thiadiazole, **T1**, 2-bromo-5-(4-bromophenyl)-1,3,4-selenadiazole, **T2**, 2-bromo-5-(4-iodophenyl)-1,3,4-selenadiazole, **T3**, and 2-bromo-5-(4-iodophenyl)-1,3,4-thiadiazole, **T4** (Fig. 1). By systematically contrasting and comparing the structural data for the compounds in this series, and by exploring the corresponding molecular electrostatic potential surfaces (MEPS), Hirshfeld surfaces and energy frameworks, we hope to be able to fine-tune the balance between different intermolecular interactions and learn the main contributing factors in the structural arrangements, thus enabling us to tailor-make properties of 1,3,4-chalcogenadiazoles.

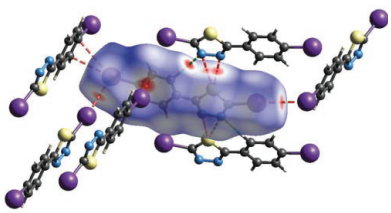

Table 1
Experimental details.

	T1	T2	T3	T4
Crystal data				
Chemical formula	$C_8H_4I_2N_2S$	$C_8H_4Br_2N_2Se$	$C_8H_4BrIN_2Se$	$C_8H_4BrIN_2S$
M_r	413.99	366.91	413.90	367.00
Crystal system, space group	Orthorhombic, *Pbca*	Orthorhombic, *Pbca*	Orthorhombic, *Pbca*	Orthorhombic, *Pbca*
Temperature (K)	293	100	100	293
a, *b*, *c* (Å)	11.0392 (2), 8.1756 (2), 23.3673 (4)	11.1945 (5), 7.1006 (3), 25.4725 (9)	11.1735 (4), 7.1222 (2), 26.1875 (8)	10.9919 (2), 6.9945 (1), 26.4076 (4)
V (Å^3)	2108.95 (7)	2024.74 (15)	2084.00 (11)	2030.29 (6)
Z	8	8	8	8
Radiation type	Cu $K\alpha$	Cu $K\alpha$	Mo $K\alpha$	Cu $K\alpha$
μ (mm^{-1})	48.34	13.90	10.36	30.95
Crystal size (mm)	0.07 × 0.05 × 0.03	0.02 × 0.02 × 0.02	0.3 × 0.1 × 0.06	0.05 × 0.04 × 0.01
Data collection				
Diffractometer	Rigaku XtaLAB Synergy Custom diffractometer with a HyPix-Arc 150° detector	Rigaku XtaLAB Synergy Custom diffractometer with a HyPix-Arc 150° detector	Rigaku XtaLAB Synergy Custom diffractometer with a HyPix-Arc 150° detector	Rigaku XtaLAB Synergy Custom diffractometer with a HyPix-Arc 150° detector
Absorption correction	Gaussian (*CrysAlis PRO*; Rigaku OD, 2020)	Multi-scan (*CrysAlis PRO*; Rigaku OD, 2020)	Multi-scan (*CrysAlis PRO*; Rigaku OD, 2020)	Multi-scan (*CrysAlis PRO*; Rigaku OD, 2020)
T_{min}, T_{max}	0.209, 0.522	0.682, 1.000	0.338, 1.000	0.373, 1.000
No. of measured, independent and observed [$I > 2\sigma(I)$] reflections	8336, 1942, 1753	6457, 1965, 1709	12091, 2055, 1815	7258, 1920, 1802
R_{int}	0.024	0.037	0.035	0.025
$(\sin\theta/\lambda)_{max}$ (Å^{-1})	0.606	0.625	0.617	0.612
Refinement				
$R[F^2 > 2\sigma(F^2)]$, $wR(F^2)$, S	0.026, 0.071, 1.09	0.044, 0.109, 1.05	0.030, 0.070, 1.08	0.021, 0.052, 1.07
No. of reflections	1942	1965	2055	1920
No. of parameters	118	118	118	118
H-atom treatment	H-atom parameters constrained	H-atom parameters constrained	H-atom parameters constrained	H-atom parameters constrained
$\Delta\rho_{max}$, $\Delta\rho_{min}$ (e Å^{-3})	1.33, −1.22	1.95, −1.46	2.00, −1.01	0.57, −0.67

Computer programs: *CrysAlis PRO* (Rigaku OD, 2020), *SHELXT2018* (Sheldrick, 2015*a*), *SHELXL2018* (Sheldrick, 2015*b*), and *OLEX2* (Dolomanov *et al.*, 2009).

2. Experimental

2.1. Materials and methods

All amine starting materials were synthesized based on previously reported procedures and were purified by column chromatography (De Silva *et al.*, 2021). Isopentyl nitrite (iAmONO), sodium nitrite, copper(I) bromide, elemental iodine, and hydrobromic acid were purchased from Fischer Scientific and used without further purification.

2.2. General synthesis of the iodo analogues

The targets were synthesized (Fig. 2) using conditions modified from reported procedures (Barbachyn, 2006). The relevant amine (*ca* 1 mmol) was dissolved in acetonitrile (4 ml) and dichloromethane (1 ml), and the resulting solution cooled to 0 °C. To this, isopentyl nitrite (0.4 ml) was added, followed by the addition of iodine (1 mmol) in acetonitrile. Dimethylformamide (1–2 ml) was added to the mixture, which was stirred overnight. To this, saturated $NaHSO_3$ was added and the product was extracted with dichloromethane (DCM). The organic layer was washed with brine, dried over magnesium sulfate, and concentrated. The crude product was washed with diethyl ether to obtain the pure product, which was characterized by NMR spectroscopy.

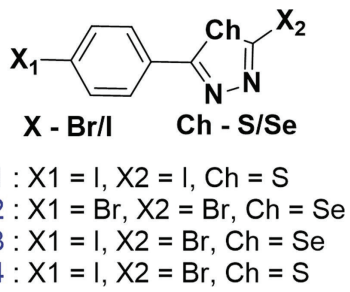

Figure 1
The target library of chalcogenadiazole derivatives, showing the structures of **T1**–**T4**.

2.3. General synthesis of the bromo analogues

The targets were synthesized (Fig. 3) using conditions modified from reported procedures (Walker, 2017). The amine starting material (1 mmol) was added to a stirred solution of

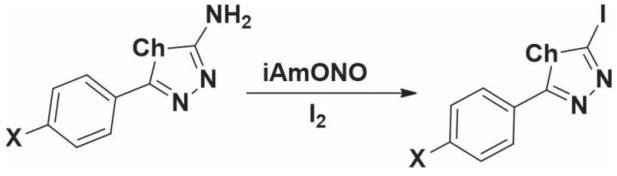

Figure 2
The reaction conditions for replacing an amine group with iodine.

Figure 3
The reaction conditions for replacing an amine group with bromine.

excess hydrobromic acid (15 mmol) at room temperature and water (2 ml) was added to the resulting slurry. This mixture was cooled to 0 °C in an ice bath and copper(I) bromide (1 mmol) was added. Sodium nitrite (1.2 mmol) was dissolved in water (2 ml) and added to the slurry dropwise, followed by stirring for another 30 min. The mixture was neutralized with saturated sodium bicarbonate and the product extracted with DCM. The organic layer was dried and the product was purified with column chromatography and characterized by NMR spectroscopy.

2.4. Crystallization

The pure materials were dissolved in either tetrahydrofuran or dioxane, followed by slow evaporation to obtain single crystals within 2–5 d.

2.5. Refinement

Crystal data, data collection and structure refinement details are summarized in Table 1. H atoms were placed geometrically and refined using riding model.

Table 2
Halogen- and chalcogen-bond geometries (Å, °).

Target	*R*—*D*···*A*	*D*···*A*	*R*—*D*···*A*
T1	I12···I13	3.7477 (6)	174.33 (12)
	I13···C3	3.368 (4)	89.8 (3)
	S11···N8	3.147 (4)	143.32 (17)
	S11···N9	3.236 (4)	157.99 (19)
	C2—H2···N9	3.478 (6)	121.2 (5)
T2	Br12···Br13	3.4685 (10)	169.11 (17)
	Se11···N8	3.060 (5)	146.97 (19)
	Se11···N9	3.123 (5)	157.99 (19)
	C2—H2···N9	3.690 (8)	121.2 (5)
T3	Br12···I13	3.6237 (7)	168.76 (13)
	Se11···N8	3.050 (3)	146.11 (15)
	Se11···N9	3.129 (3)	158.18 (15)
	C2—H2···N9	3.696 (6)	121.1 (3)
T4	Br12···I13	3.6141 (7)	170.09 (11)
	S11···N8	3.071 (2)	147.59 (12)
	S11···N9	3.153 (2)	151.79 (12)
	C2—H2···N9	3.646 (4)	122.5 (2)

3. Results and discussion

3.1. Crystal structures

Compounds **T1**–**T4** all crystallized in the space group *Pbca* and were isostructural. In the structure of **T1**, the I atom at the 2-position of the chalcogenadiazole ring forms a halogen bond (XB) in which the I atom in the *para* position of the arene ring acts as the XB acceptor, which leads to a zigzag arrangement in the crystal structure (Fig. 4). This type of XB can be observed for all the targets reported in this study. The *para*-halogen atoms display, in all cases except for **T1**, short contacts with the π-electron cloud on the arene ring, as the molecular structure does not facilitate conventional XB formation. In **T1**, however, the geometrical features allow the *para*-I atom to

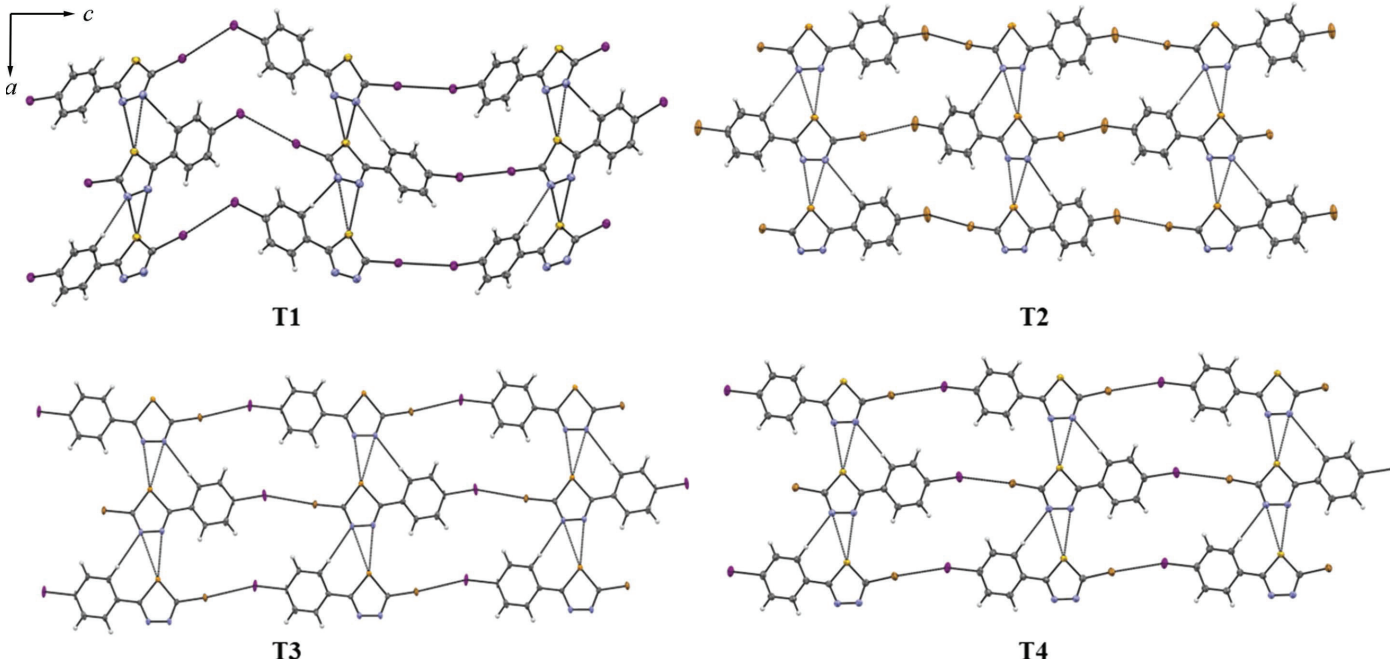

Figure 4
Significant noncovalent interactions shown in isostructural analogues **T1**–**T4**. The S and Se atoms both display chalcogen bonding (ChB) between the two N atoms.

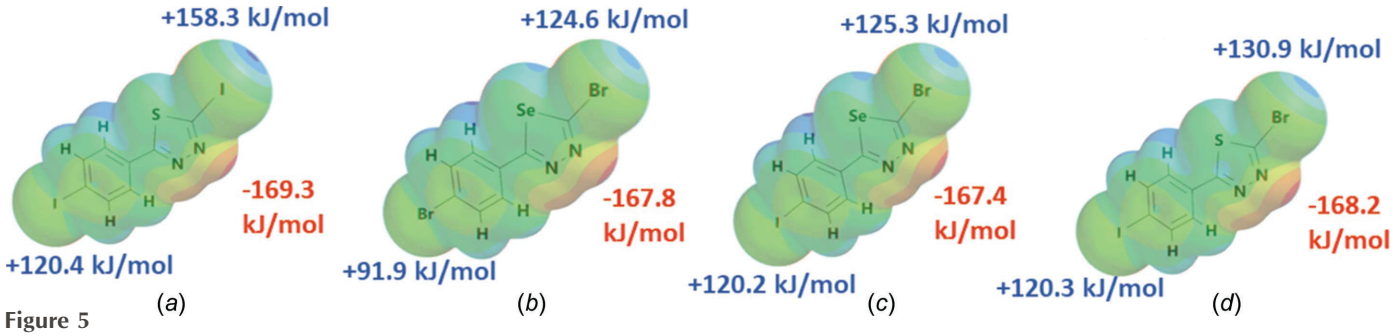

Figure 5
Molecular electrostatic potential surfaces (MEPS) of **T1**–**T4**.

form an XB with the π-electron cloud of the arene ring, leading to a more compact crystal packing (Fig. S5 in the supporting information).

The S and Se atoms both displayed chalcogen bonding (ChB) to the two N atoms of the heterocycle, resulting in bifurcated interactions. In general, the Se atom showed shorter ChB bond distances compared to its S counterpart. All relevant bond distances and angles are given in Table 2.

3.2. Molecular electrostatic potential surfaces (MEPS)

MEPS have been used to determine σ-hole potentials and to successfully evaluate their competing nature in many different systems (Politzer & Murray, 2021; Aakeröy *et al.*, 2016). Here the electrostatic potentials were calculated at the B3LYP/6-311G**++ level of theory using *Spartan'14* (Hehre, 2003). A summary of these results for **T1**–**T4** is shown in Fig. 5. Based on the MEPs, it was clear that the halogen atoms in the 2-position of the chalcogenadiazole ring presented larger σ-hole potentials compared to those when the halogen atom was in the *para* position. Halogen atoms on the 2-position of the thiadiazole species had the highest σ-hole potential for both Br and I due to sulfur being more electronegative than selenium. Among the chalcogen atoms, as expected, the more polarizable Se atom showed a larger σ-hole compared to the S atom. The areas of positive electrostatic potential were largely positioned directly opposite the C—Ch bond, but the σ-hole closest to the arene ring contains an area of positive potential which has been overlapped with the positive potential of the C—H group, which is similar to what was observed recently for the benzothiazolium species (Konidaris *et al.*, 2022).

The most negative electrostatic potential was observed for the N atom in the 3-position, which would then be viewed as the best acceptor for a σ-hole bond donor. The second and third largest negative potentials were observed for the lone pairs of the halogen atoms and the π-electron cloud. XB formation was observed between the best donor and the second- and third-best acceptors, while the ChB was between the second-best donor and the best acceptor.

3.3. Hirshfeld surface analysis

The Hirshfeld surfaces and fingerprint plots (Spackman & Jayatilaka, 2009) were generated for **T1**–**T4** using *CrystalExplorer17.5* (Spackman *et al.*, 2021) in order to study the key intermolecular interactions driving the structural arrangement. Hirshfeld surface two-dimensional (2D) fingerprint plots showed major contributions arising from I···H/H···I and Br···H/H···Br contacts, regardless of the structural positioning; however, with respect to the structure-directing interactions, they indicated that the most dominant interactions were halogen and chalcogen bonds. For **T1**, the halogen contacts observed were I···I (8%) and I···C/C···I (8.2%), and for **T2**, the dominant interactions were Br···Br (10.6%) and Br···C/C···Br (3.2%). For both **T3** and **T4**, there were I···Br/Br···I (7.5 and 6.7%, respectively) and I···C/C···I (1 and 1.8%) contacts.

In the case of chalcogen bonding, **T1** and **T4** showed S···N/N···S (4.4 and 7.2%, respectively), while **T2** and **T3** had Se···N/N···Se (6.8 and 6.8%) contacts. These bifurcated ChB are directed more toward the N atoms; hence, the ChB configuration deviated slightly from an ideal ChB which forms along the C—Ch axis. Interestingly, the only non-σ-hole interaction present was C—H···N hydrogen bonding (HB) (3.2, 2.7, and 2.8% for **T1**, **T2**–**T3**, and **T4**, respectively), which was observed for all four targets (Figs. 6 and 7).

Furthermore, the total Hirshfeld surfaces for **T1**–**T4** were very similar, except for the regions of XB interaction. For **T1** and **T2**, only one region was observed, as both halogen atoms present were the same, but as for **T3** and **T4**, there were mainly three regions of significance (Fig. 8).

3.4. Energy frameworks

To further explore the competition among these noncovalent interactions, the energy frameworks for **T1**–**T4** were

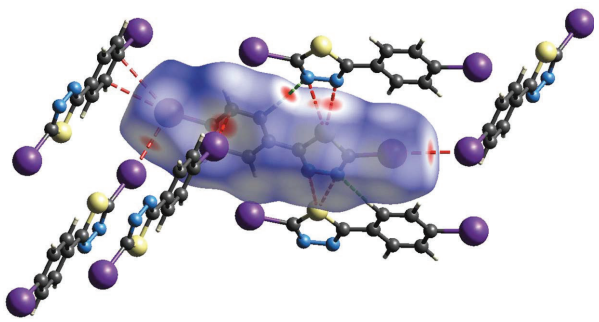

Figure 6
Hirshfeld surface mapped over d_{norm} for **T1**.

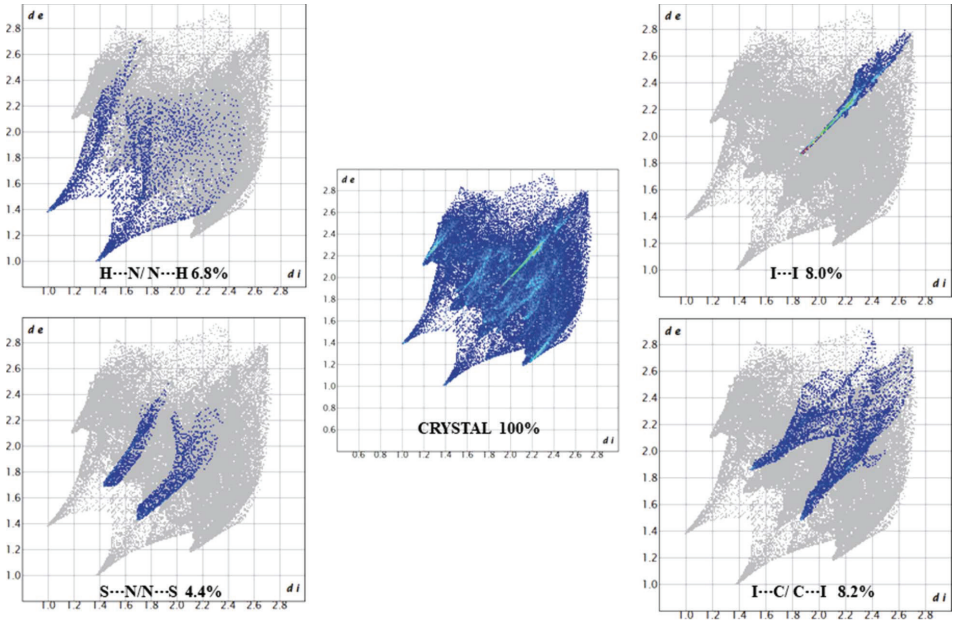

Figure 7
2D fingerprint plots of **T1** for the observed noncovalent interactions.

generated using *TONTO* B3LYP/6-311G(d,p) (Mackenzie *et al.*, 2017) for **T2** and B3LYP/DGDZVP (Torubaev & Samigullina, 2022; Speetzen *et al.*, 2022; Mackenzie *et al.*, 2017) for the other three iodine species (Fig. 9). Based on the energy framework obtained for **T1**, the ChB acts as a strong Coulombic interaction between the molecules when compared to the XB, which explains the interaction of the second-best donor with the best acceptor according to the MEPS. This confirms the fact that the formation of the bifurcated ChB is more influential than the individual XBs that were formed. The dispersion interactions showed the presence of π–π stacking between the aromatic rings, which greatly contributes to the stabilization of the crystal lattice. Energy frameworks for the other three targets can be found in Figs. S6–S8 of the supporting information.

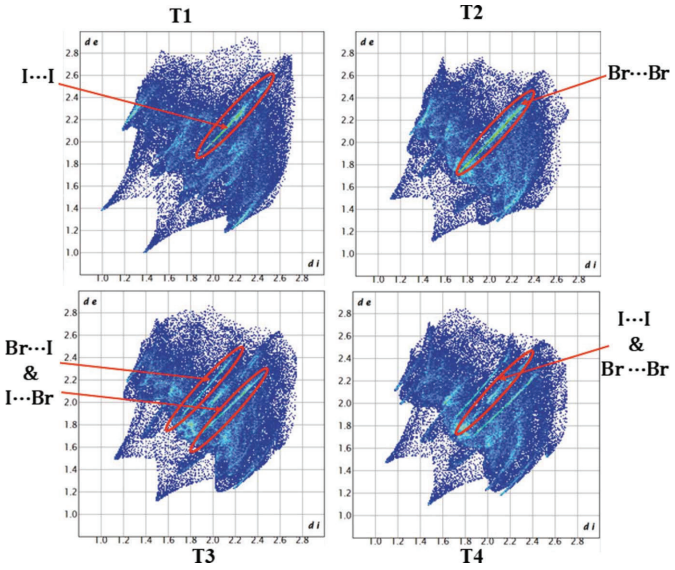

Figure 8
Total Hirshfeld surfaces for **T1**–**T4** highlighting the fingerprint regions of halogen bonding.

4. Conclusion

In this study, four isostructural chalcogenadiazole derivatives have been synthesized, characterized, and analyzed using SC-XRD, MEPS, and Hirshfeld surfaces. The MEP data showed that the halogen atoms at the 2-position of the chalcogenadiazole ring had a larger σ-hole than the *para* halogen atoms, which made them better XB donors with increased directionality. Hirshfeld surfaces showed a stronger structural influence for noncovalent interactions arising from I···I and Br···Br of **T1** and **T2**, respectively, in comparison with **T3** and **T4**, where the two halogen atoms on opposite ends of the molecule were different. Overall, however, the relative percentage contribution of the I···Br/Br···I contacts of **T3** and **T4** was between those found in **T1** and **T2**. Though MEPS predicted that the halogens with the larger σ-hole should form XB with the best-acceptor N atom, the diazo N atoms form ChBs with the second-best donor Ch instead of the halogen, forming bifurcated ChBs for all four structures, with the Se compounds, in general, showing shorter Ch···N contacts than the S compounds. Thus, it can be concluded that for these isostructural species, ChB has won the competition between XB and ChB.

Acknowledgements

The authors acknowledge an NSF–MRI grant, which was used to purchase the single-crystal X-ray diffractometer and the associated software employed in this study. VDS acknowl-

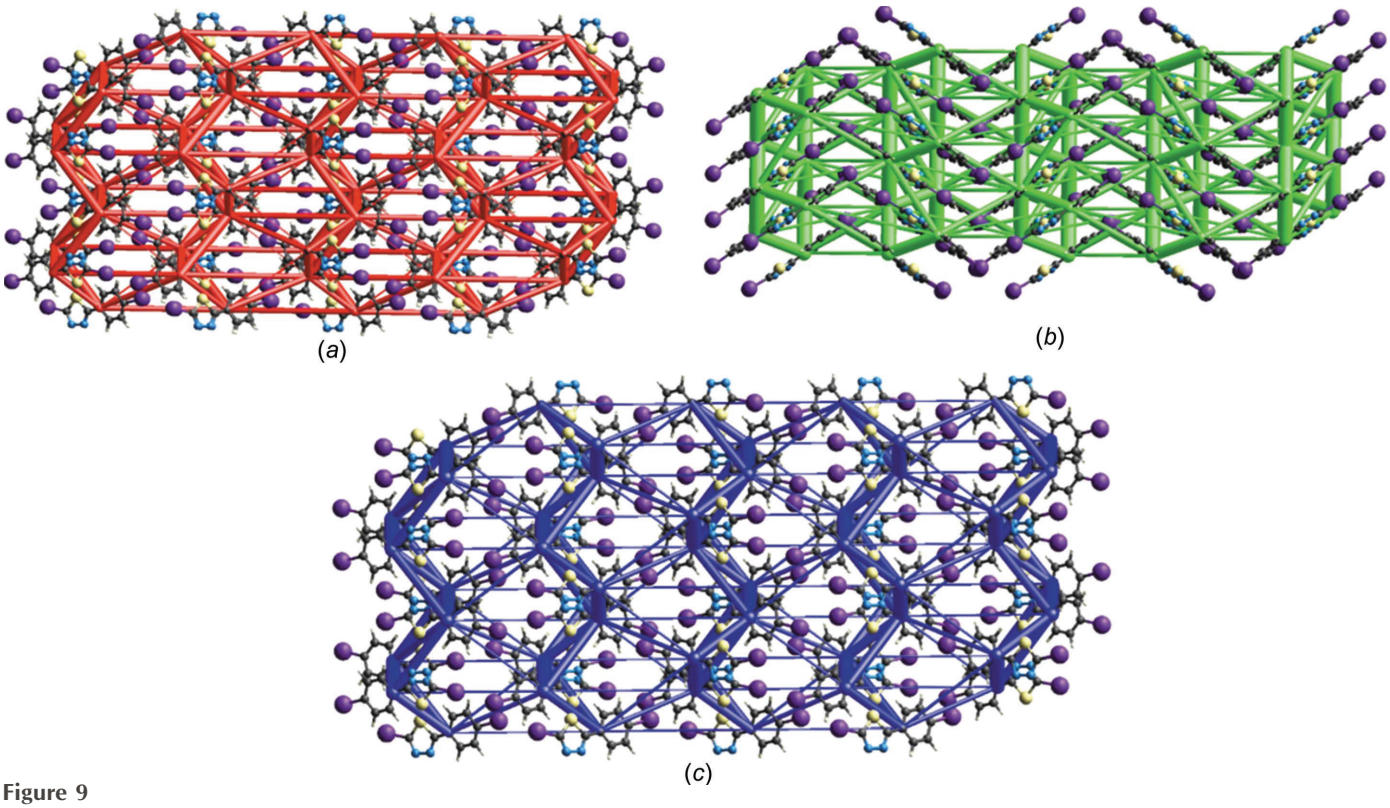

Figure 9
Energy framework calculations showing (*a*) the Coulombic interactions, (*b*) the dispersion interactions and (*c*) the total interaction energies of **T1**, in which the line thickness represents the relative strength of the energy component.

edges support from the Johnson Cancer Research Center at Kansas State University.

Funding information

Funding for this research was provided by: National Science Foundation, Major Research Instrumentation Program (grant No. CHE-2018414).

References

Aakeröy, C. B., Wijethunga, T. K., Desper, J. & Đaković, M. (2016). *Cryst. Growth Des.* **16**, 2662–2670.
Barbachyn, M. (2006). Antibacterial Agents. (International Publication Number WO 2006/120563 A2.)
De Silva, V., Averkiev, B. B., Sinha, A. S. & Aakeröy, C. B. (2021). *Molecules*, **26**, 4125.
Dolomanov, O. V., Bourhis, L. J., Gildea, R. J., Howard, J. A. K. & Puschmann, H. (2009). *J. Appl. Cryst.* **42**, 339–341.
Genis, C., Sippel, K. H., Case, N., Cao, W., Avvaru, B. S., Tartaglia, L. J., Govindasamy, L., Tu, C., Agbandje-McKenna, M., Silverman, D. N., Rosser, C. J. & McKenna, R. (2009). *Biochemistry*, **48**, 1322–1331.
Hehre, W. J. (2003). In *A Guide to Molecular Mechanics and Quantum Chemical Calculations*. Irvine, CA: Wavefunction Inc.
Hu, Y., Li, C. Y., Wang, X. M., Yang, Y. H. & Zhu, H. L. (2014). *Chem. Rev.* **114**, 5572–5610.
Konidaris, K., Daolio, A., Pizzi, A., Scilabra, P., Terraneo, G., Quici, S., Murray, J. S., Politzer, P. & Resnati, G. (2022). *Cryst. Growth Des.* **22**, 4987–4995.
Kumar, H., Javed, S. A., Khan, S. A. & Amir, M. (2008). *Eur. J. Med. Chem.* **43**, 2688–2698.
Mackenzie, C. F., Spackman, P. R., Jayatilaka, D. & Spackman, M. A. (2017). *IUCrJ*, **4**, 575–587.
Politzer, P. & Murray, J. S. (2021). In *Chemical Reactivity in Confined Systems*, edited by P. K. Chattaraj & D. Chakraborty, pp. 113–134. Chichester; John Wiley & Sons Ltd.
Rigaku OD (2020). *CrysAlis PRO*. Rigaku Oxford Diffraction Ltd, Yarnton, Oxfordshire, England.
Sheldrick, G. M. (2015*a*). *Acta Cryst.* A**71**, 3–8.
Sheldrick, G. M. (2015*b*). *Acta Cryst.* C**71**, 3–8.
Spackman, M. A. & Jayatilaka, D. (2009). *CrystEngComm*, **11**, 19–32.
Spackman, P. R., Turner, M. J., McKinnon, J. J., Wolff, S. K., Grimwood, D. J., Jayatilaka, D. & Spackman, M. A. (2021). *J. Appl. Cryst.* **54**, 1006–1011.
Speetzen, E. D., Nwachukwu, C. I., Bowling, N. P. & Bosch, E. (2022). *Molecules*, **27**, 1527.
Torubaev, Y. V. & Samigullina, A. S. (2022). *Chemistry*, **4**, 196–205.
Walker, K. (2017). Biosynthesis of Paclitaxel Intermediate. (International Publication Number WO 2017/011214 A1.)

supporting information

Acta Cryst. (2022). C**78**, 716-721 [https://doi.org/10.1107/S205322962201052X]

Competition between chalcogen and halogen bonding assessed through isostructural species

Viraj De Silva, Pierre Le Magueres, Boris B. Averkiev and Christer B. Aakeröy

Computing details

Data collection: *CrysAlis PRO* (Rigaku OD, 2020) for T1, T4; *CrysAlis PRO* 1.171.41.76a (Rigaku OD, 2020) for T2; *CrysAlis PRO* 1.171.40.84a (Rigaku OD, 2020) for T3. Cell refinement: *CrysAlis PRO* (Rigaku OD, 2020) for T1, T4; *CrysAlis PRO* 1.171.41.76a (Rigaku OD, 2020) for T2; *CrysAlis PRO* 1.171.40.84a (Rigaku OD, 2020) for T3. Data reduction: *CrysAlis PRO* (Rigaku OD, 2020) for T1, T4; *CrysAlis PRO* 1.171.41.76a (Rigaku OD, 2020) for T2; *CrysAlis PRO* 1.171.40.84a (Rigaku OD, 2020) for T3. Program(s) used to solve structure: SHELXT2018 (Sheldrick, 2015*a*) for T1; SHELXT (Sheldrick, 2015*a*) for T2, T3, T4. For all structures, program(s) used to refine structure: *SHELXL2018* (Sheldrick, 2015*b*); molecular graphics: OLEX2 (Dolomanov *et al.*, 2009); software used to prepare material for publication: OLEX2 (Dolomanov *et al.*, 2009).

2-Iodo-5-(4-iodophenyl)-1,3,4-thiadiazole (T1)

Crystal data

$C_8H_4I_2N_2S$
M_r = 413.99
Orthorhombic, *Pbca*
a = 11.0392 (2) Å
b = 8.1756 (2) Å
c = 23.3673 (4) Å
V = 2108.95 (7) Å^3
Z = 8
F(000) = 1504
D_x = 2.608 Mg m^{-3}
Cu *Kα* radiation, *λ* = 1.54184 Å
Cell parameters from 5508 reflections
θ = 3.8–69.0°
μ = 48.34 mm^{-1}
T = 293 K
Block, colourless
0.07 × 0.05 × 0.03 mm

Data collection

Rigaku XtaLAB Synergy Custom diffractometer with a HyPix-Arc 150° detector
Radiation source: Rotating-anode X-ray tube, Rigaku (Cu) X-ray Source
Mirror monochromator
Detector resolution: 10.0000 pixels mm^{-1}
ω scans
Absorption correction: gaussian (CrysAlis PRO; Rigaku OD, 2020)
T_{min} = 0.209, T_{max} = 0.522
8336 measured reflections
1942 independent reflections
1753 reflections with $I > 2\sigma(I)$
R_{int} = 0.024
θ_{max} = 69.1°, θ_{min} = 3.8°
h = −11→13
k = −8→9
l = −24→28

Refinement

Refinement on F^2
Least-squares matrix: full
$R[F^2 > 2\sigma(F^2)]$ = 0.026
$wR(F^2)$ = 0.071
S = 1.09
1942 reflections
118 parameters
0 restraints

Primary atom site location: dual
Hydrogen site location: inferred from neighbouring sites
H-atom parameters constrained

$w = 1/[\sigma^2(F_o^2) + (0.0388P)^2 + 4.6153P]$ where $P = (F_o^2 + 2F_c^2)/3$
$(\Delta/\sigma)_{max} = 0.001$
$\Delta\rho_{max} = 1.33$ e Å^{-3}
$\Delta\rho_{min} = -1.22$ e Å^{-3}

Special details

Geometry. All esds (except the esd in the dihedral angle between two l.s. planes) are estimated using the full covariance matrix. The cell esds are taken into account individually in the estimation of esds in distances, angles and torsion angles; correlations between esds in cell parameters are only used when they are defined by crystal symmetry. An approximate (isotropic) treatment of cell esds is used for estimating esds involving l.s. planes.

Fractional atomic coordinates and isotropic or equivalent isotropic displacement parameters (Å²)

	x	*y*	*z*	U_{iso}*/U_{eq}
C1	0.6455 (4)	0.4015 (5)	0.40675 (18)	0.0196 (9)
C2	0.5284 (4)	0.4540 (6)	0.39544 (19)	0.0209 (9)
H2	0.465059	0.421230	0.419049	0.025*
C3	0.5054 (4)	0.5556 (5)	0.34887 (18)	0.0207 (9)
H3	0.427089	0.591795	0.341467	0.025*
C4	0.6006 (4)	0.6024 (5)	0.31353 (18)	0.0218 (9)
C5	0.7186 (4)	0.5514 (5)	0.32447 (19)	0.0245 (10)
H5	0.782009	0.584936	0.301019	0.029*
C6	0.7402 (4)	0.4498 (6)	0.37097 (18)	0.0219 (9)
H6	0.818500	0.413535	0.378344	0.026*
C7	0.6712 (4)	0.2974 (5)	0.45654 (18)	0.0205 (9)
N8	0.7801 (3)	0.2525 (4)	0.47101 (17)	0.0242 (9)
N9	0.7827 (3)	0.1583 (5)	0.52011 (16)	0.0243 (8)
C10	0.6745 (4)	0.1372 (5)	0.54045 (18)	0.0212 (9)
S11	0.55940 (10)	0.22850 (15)	0.50283 (5)	0.0246 (3)
I12	0.64084 (3)	0.00912 (3)	0.61590 (2)	0.02546 (12)
I13	0.56375 (3)	0.75148 (3)	0.24272 (2)	0.02576 (12)

Atomic displacement parameters (Å²)

	U^{11}	U^{22}	U^{33}	U^{12}	U^{13}	U^{23}
C1	0.021 (2)	0.018 (2)	0.020 (2)	0.0000 (17)	0.0006 (17)	−0.0003 (18)
C2	0.019 (2)	0.020 (2)	0.023 (2)	−0.0004 (18)	0.0016 (18)	−0.0021 (18)
C3	0.021 (2)	0.020 (2)	0.021 (2)	0.0020 (18)	0.0001 (18)	0.0002 (18)
C4	0.028 (2)	0.0163 (19)	0.021 (2)	0.0016 (18)	0.0005 (19)	−0.0001 (17)
C5	0.027 (2)	0.019 (2)	0.027 (2)	−0.0020 (19)	0.0067 (18)	−0.0058 (19)
C6	0.021 (2)	0.017 (2)	0.028 (2)	−0.0010 (18)	0.0026 (19)	−0.0052 (18)
C7	0.022 (2)	0.019 (2)	0.020 (2)	−0.0014 (18)	−0.0009 (18)	0.0002 (18)
N8	0.021 (2)	0.027 (2)	0.0241 (19)	0.0015 (16)	−0.0022 (15)	0.0023 (16)
N9	0.024 (2)	0.027 (2)	0.0223 (17)	0.0037 (17)	−0.0021 (16)	0.0015 (16)
C10	0.022 (2)	0.018 (2)	0.024 (2)	0.0003 (18)	−0.0040 (19)	−0.0023 (18)
S11	0.0187 (6)	0.0283 (6)	0.0267 (6)	0.0013 (4)	−0.0004 (4)	0.0053 (5)
I12	0.0279 (2)	0.02557 (18)	0.02293 (18)	0.00177 (11)	−0.00234 (11)	0.00194 (11)
I13	0.0349 (2)	0.02059 (18)	0.02173 (18)	−0.00176 (11)	−0.00195 (11)	0.00162 (11)

Geometric parameters (Å, º)

C1—C2	1.388 (6)	C5—H5	0.9300
C1—C6	1.395 (6)	C5—C6	1.389 (6)
C1—C7	1.469 (6)	C6—H6	0.9300
C2—H2	0.9300	C7—N8	1.302 (6)
C2—C3	1.392 (6)	C7—S11	1.735 (4)
C3—H3	0.9300	N8—N9	1.382 (5)
C3—C4	1.390 (6)	N9—C10	1.297 (6)
C4—C5	1.391 (6)	C10—S11	1.716 (4)
C4—I13	2.095 (4)	C10—I12	2.084 (4)
C2—C1—C6	119.7 (4)	C6—C5—H5	120.5
C2—C1—C7	120.6 (4)	C1—C6—H6	119.7
C6—C1—C7	119.6 (4)	C5—C6—C1	120.7 (4)
C1—C2—H2	119.9	C5—C6—H6	119.7
C1—C2—C3	120.2 (4)	C1—C7—S11	123.0 (3)
C3—C2—H2	119.9	N8—C7—C1	123.2 (4)
C2—C3—H3	120.3	N8—C7—S11	113.8 (3)
C4—C3—C2	119.4 (4)	C7—N8—N9	113.1 (4)
C4—C3—H3	120.3	C10—N9—N8	111.1 (3)
C3—C4—C5	121.1 (4)	N9—C10—S11	115.9 (3)
C3—C4—I13	118.8 (3)	N9—C10—I12	122.8 (3)
C5—C4—I13	120.1 (3)	S11—C10—I12	121.3 (2)
C4—C5—H5	120.5	C10—S11—C7	86.2 (2)
C6—C5—C4	118.9 (4)		
C1—C2—C3—C4	0.7 (7)	C6—C1—C7—S11	−179.0 (3)
C1—C7—N8—N9	178.4 (4)	C7—C1—C2—C3	178.6 (4)
C1—C7—S11—C10	−178.5 (4)	C7—C1—C6—C5	−178.4 (4)
C2—C1—C6—C5	0.7 (7)	C7—N8—N9—C10	−0.1 (5)
C2—C1—C7—N8	−175.9 (4)	N8—C7—S11—C10	−0.4 (4)
C2—C1—C7—S11	1.9 (6)	N8—N9—C10—S11	−0.2 (5)
C2—C3—C4—C5	−1.0 (6)	N8—N9—C10—I12	−177.7 (3)
C2—C3—C4—I13	178.8 (3)	N9—C10—S11—C7	0.3 (4)
C3—C4—C5—C6	1.2 (6)	S11—C7—N8—N9	0.4 (5)
C4—C5—C6—C1	−1.0 (7)	I12—C10—S11—C7	177.9 (3)
C6—C1—C2—C3	−0.5 (7)	I13—C4—C5—C6	−178.6 (3)
C6—C1—C7—N8	3.2 (7)		

2-Bromo-5-(4-bromophenyl)-1,3,4-selenadiazole (T2)

Crystal data

$C_8H_4Br_2N_2Se$
M_r = 366.91
Orthorhombic, *Pbca*
a = 11.1945 (5) Å
b = 7.1006 (3) Å
c = 25.4725 (9) Å
V = 2024.74 (15) Å^3
Z = 8
F(000) = 1360
D_x = 2.407 Mg m^{-3}
Cu *Kα* radiation, *λ* = 1.54184 Å
Cell parameters from 3007 reflections
θ = 3.5–74.7°
μ = 13.90 mm^{-1}

T = 100 K
Irregular, orange

0.02 × 0.02 × 0.02 mm

Data collection

Rigaku XtaLAB Synergy Custom diffractometer with a HyPix-Arc 150° detector
Radiation source: micro-focus sealed X-ray tube, PhotonJet (Cu) X-ray Source
Mirror monochromator
Detector resolution: 10.0000 pixels mm^{-1}
ω scans
Absorption correction: multi-scan (CrysAlis PRO; Rigaku OD, 2020)

T_{min} = 0.682, T_{max} = 1.000
6457 measured reflections
1965 independent reflections
1709 reflections with $I > 2\sigma(I)$
R_{int} = 0.037
θ_{max} = 74.8°, θ_{min} = 3.5°
h = −9→13
k = −8→8
l = −29→30

Refinement

Refinement on F^2
Least-squares matrix: full
$R[F^2 > 2\sigma(F^2)]$ = 0.044
$wR(F^2)$ = 0.109
S = 1.05
1965 reflections
118 parameters
0 restraints
Primary atom site location: dual

Hydrogen site location: inferred from neighbouring sites
H-atom parameters constrained
$w = 1/[\sigma^2(F_o^2) + (0.0428P)^2 + 15.9376P]$ where $P = (F_o^2 + 2F_c^2)/3$
$(\Delta/\sigma)_{max}$ = 0.001
$\Delta\rho_{max}$ = 1.95 e Å^{-3}
$\Delta\rho_{min}$ = −1.46 e Å^{-3}

Special details

Geometry. All esds (except the esd in the dihedral angle between two l.s. planes) are estimated using the full covariance matrix. The cell esds are taken into account individually in the estimation of esds in distances, angles and torsion angles; correlations between esds in cell parameters are only used when they are defined by crystal symmetry. An approximate (isotropic) treatment of cell esds is used for estimating esds involving l.s. planes.

Fractional atomic coordinates and isotropic or equivalent isotropic displacement parameters (Å^2)

	x	y	z	U_{iso}*/U_{eq}
C1	0.3302 (5)	0.3834 (8)	0.5943 (2)	0.0221 (12)
C2	0.4462 (6)	0.4100 (9)	0.6138 (2)	0.0281 (13)
H2	0.513177	0.382973	0.592141	0.034*
C3	0.4634 (7)	0.4753 (9)	0.6643 (3)	0.0350 (15)
H3	0.541775	0.495041	0.677551	0.042*
C4	0.3654 (7)	0.5113 (9)	0.6952 (2)	0.0329 (15)
C5	0.2498 (7)	0.4874 (8)	0.6768 (2)	0.0316 (14)
H5	0.183353	0.515334	0.698698	0.038*
C6	0.2326 (6)	0.4222 (8)	0.6263 (2)	0.0276 (13)
H6	0.153883	0.403931	0.613314	0.033*
C7	0.3101 (5)	0.3151 (8)	0.5401 (2)	0.0180 (11)
N8	0.2045 (4)	0.2908 (7)	0.52118 (18)	0.0227 (10)
N9	0.2012 (4)	0.2252 (7)	0.46988 (18)	0.0227 (10)
C10	0.3064 (5)	0.2028 (8)	0.4508 (2)	0.0211 (12)
Se11	0.43492 (5)	0.25540 (9)	0.49395 (2)	0.02259 (19)
Br12	0.32759 (6)	0.11997 (9)	0.38120 (2)	0.0301 (2)
Br13	0.39006 (10)	0.60799 (12)	0.76394 (3)	0.0541 (3)

Atomic displacement parameters (Å²)

	U^{11}	U^{22}	U^{33}	U^{12}	U^{13}	U^{23}
C1	0.033 (3)	0.017 (3)	0.016 (3)	0.000 (2)	−0.001 (2)	0.002 (2)
C2	0.036 (3)	0.030 (3)	0.018 (3)	−0.008 (3)	−0.002 (3)	0.009 (2)
C3	0.048 (4)	0.031 (3)	0.026 (3)	−0.007 (3)	−0.010 (3)	0.007 (3)
C4	0.059 (4)	0.026 (3)	0.014 (3)	−0.003 (3)	−0.002 (3)	0.004 (2)
C5	0.053 (4)	0.018 (3)	0.023 (3)	0.005 (3)	0.008 (3)	0.002 (3)
C6	0.034 (3)	0.020 (3)	0.028 (3)	0.004 (3)	0.000 (3)	0.002 (2)
C7	0.017 (3)	0.013 (2)	0.024 (3)	0.002 (2)	−0.001 (2)	0.002 (2)
N8	0.023 (2)	0.027 (3)	0.018 (2)	−0.002 (2)	0.0004 (19)	0.005 (2)
N9	0.024 (2)	0.024 (3)	0.020 (2)	−0.003 (2)	−0.0022 (19)	0.002 (2)
C10	0.026 (3)	0.017 (3)	0.020 (3)	−0.003 (2)	0.002 (2)	0.001 (2)
Se11	0.0167 (3)	0.0242 (3)	0.0269 (3)	−0.0007 (2)	0.0013 (2)	−0.0020 (2)
Br12	0.0405 (4)	0.0285 (3)	0.0213 (3)	−0.0041 (3)	0.0050 (3)	−0.0039 (3)
Br13	0.1013 (8)	0.0407 (4)	0.0205 (3)	−0.0056 (5)	−0.0081 (4)	−0.0012 (3)

Geometric parameters (Å, º)

C1—C2	1.403 (9)	C5—H5	0.9500
C1—C6	1.391 (9)	C5—C6	1.382 (8)
C1—C7	1.479 (8)	C6—H6	0.9500
C2—H2	0.9500	C7—N8	1.288 (7)
C2—C3	1.383 (9)	C7—Se11	1.876 (5)
C3—H3	0.9500	N8—N9	1.388 (7)
C3—C4	1.373 (10)	N9—C10	1.284 (7)
C4—C5	1.387 (10)	C10—Se11	1.849 (6)
C4—Br13	1.901 (6)	C10—Br12	1.882 (6)
C2—C1—C7	121.0 (5)	C6—C5—H5	120.5
C6—C1—C2	119.5 (5)	C1—C6—H6	119.9
C6—C1—C7	119.4 (5)	C5—C6—C1	120.2 (6)
C1—C2—H2	119.9	C5—C6—H6	119.9
C3—C2—C1	120.3 (6)	C1—C7—Se11	123.0 (4)
C3—C2—H2	119.9	N8—C7—C1	122.2 (5)
C2—C3—H3	120.5	N8—C7—Se11	114.7 (4)
C4—C3—C2	119.0 (6)	C7—N8—N9	115.0 (5)
C4—C3—H3	120.5	C10—N9—N8	112.0 (5)
C3—C4—C5	122.0 (6)	N9—C10—Se11	117.6 (4)
C3—C4—Br13	118.6 (5)	N9—C10—Br12	120.7 (4)
C5—C4—Br13	119.3 (5)	Se11—C10—Br12	121.7 (3)
C4—C5—H5	120.5	C10—Se11—C7	80.7 (2)
C6—C5—C4	119.0 (6)		
C1—C2—C3—C4	0.8 (9)	C6—C1—C7—Se11	−179.2 (4)
C1—C7—N8—N9	−179.7 (5)	C7—C1—C2—C3	179.5 (5)
C1—C7—Se11—C10	−179.8 (5)	C7—C1—C6—C5	−179.6 (5)
C2—C1—C6—C5	0.3 (9)	C7—N8—N9—C10	−0.6 (7)

C2—C1—C7—N8	−179.5 (5)	N8—C7—Se11—C10	0.6 (4)
C2—C1—C7—Se11	1.0 (8)	N8—N9—C10—Se11	1.1 (6)
C2—C3—C4—C5	−1.2 (10)	N8—N9—C10—Br12	−178.7 (4)
C2—C3—C4—Br13	−178.2 (5)	N9—C10—Se11—C7	−1.0 (5)
C3—C4—C5—C6	1.2 (9)	Se11—C7—N8—N9	−0.2 (6)
C4—C5—C6—C1	−0.7 (9)	Br12—C10—Se11—C7	178.8 (4)
C6—C1—C2—C3	−0.3 (9)	Br13—C4—C5—C6	178.1 (4)
C6—C1—C7—N8	0.3 (8)		

2-Bromo-5-(4-iodophenyl)-1,3,4-selenadiazole (T3)

Crystal data

$C_8H_4BrIN_2Se$
$M_r = 413.90$
Orthorhombic, *Pbca*
$a = 11.1735$ (4) Å
$b = 7.1222$ (2) Å
$c = 26.1875$ (8) Å
$V = 2084.00$ (11) Å^3
$Z = 8$
$F(000) = 1504$
$D_x = 2.638$ Mg m^{-3}
Mo $K\alpha$ radiation, $\lambda = 0.71073$ Å
Cell parameters from 7358 reflections
$\theta = 2.4$–$33.0°$
$\mu = 10.36$ mm^{-1}
$T = 100$ K
Plate, clear light yellow
0.3 × 0.1 × 0.06 mm

Data collection

Rigaku XtaLAB Synergy Custom diffractometer with a HyPix-Arc 150° detector
Radiation source: micro-focus sealed X-ray tube, PhotonJet (Mo) X-ray Source
Mirror monochromator
Detector resolution: 10.0000 pixels mm^{-1}
ω scans
Absorption correction: multi-scan (CrysAlis PRO; Rigaku OD, 2020)
$T_{min} = 0.338$, $T_{max} = 1.000$
12091 measured reflections
2055 independent reflections
1815 reflections with $I > 2\sigma(I)$
$R_{int} = 0.035$
$\theta_{max} = 26.0°$, $\theta_{min} = 2.4°$
$h = -13 \rightarrow 13$
$k = -7 \rightarrow 8$
$l = -32 \rightarrow 32$

Refinement

Refinement on F^2
Least-squares matrix: full
$R[F^2 > 2\sigma(F^2)] = 0.030$
$wR(F^2) = 0.070$
$S = 1.08$
2055 reflections
118 parameters
0 restraints
Primary atom site location: dual
Hydrogen site location: inferred from neighbouring sites
H-atom parameters constrained
$w = 1/[\sigma^2(F_o^2) + (0.030P)^2 + 10.0022P]$ where $P = (F_o^2 + 2F_c^2)/3$
$(\Delta/\sigma)_{max} = 0.001$
$\Delta\rho_{max} = 2.00$ e Å^{-3}
$\Delta\rho_{min} = -1.01$ e Å^{-3}

Special details

Geometry. All esds (except the esd in the dihedral angle between two l.s. planes) are estimated using the full covariance matrix. The cell esds are taken into account individually in the estimation of esds in distances, angles and torsion angles; correlations between esds in cell parameters are only used when they are defined by crystal symmetry. An approximate (isotropic) treatment of cell esds is used for estimating esds involving l.s. planes.

Fractional atomic coordinates and isotropic or equivalent isotropic displacement parameters (Å^2)

	x	*y*	*z*	U_{iso}*/U_{eq}
C1	0.6730 (4)	0.6139 (6)	0.59069 (17)	0.0149 (9)

C2	0.5578 (4)	0.5876 (7)	0.61022 (17)	0.0196 (10)
H2	0.4902	0.6141	0.5894	0.023*
C3	0.5414 (5)	0.5230 (7)	0.65978 (18)	0.0226 (10)
H3	0.4630	0.5045	0.6729	0.027*
C4	0.6408 (5)	0.4859 (6)	0.68987 (16)	0.0195 (10)
C5	0.7557 (5)	0.5112 (6)	0.67115 (17)	0.0213 (10)
H5	0.8227	0.4847	0.6923	0.026*
C6	0.7731 (4)	0.5751 (6)	0.62163 (17)	0.0176 (10)
H6	0.8518	0.5925	0.6087	0.021*
C7	0.6914 (4)	0.6814 (6)	0.53853 (16)	0.0122 (9)
N8	0.7974 (3)	0.7053 (5)	0.51957 (14)	0.0171 (8)
N9	0.8006 (3)	0.7683 (5)	0.46942 (14)	0.0184 (8)
C10	0.6957 (4)	0.7927 (6)	0.45060 (17)	0.0151 (9)
Se11	0.56664 (4)	0.74266 (7)	0.49341 (2)	0.01587 (12)
Br12	0.67471 (4)	0.87353 (7)	0.38316 (2)	0.02129 (13)
I13	0.61637 (4)	0.38409 (5)	0.76407 (2)	0.03129 (12)

Atomic displacement parameters (Å²)

	U^{11}	U^{22}	U^{33}	U^{12}	U^{13}	U^{23}
C1	0.021 (2)	0.009 (2)	0.015 (2)	0.0004 (18)	0.0006 (17)	−0.0032 (17)
C2	0.024 (2)	0.020 (2)	0.015 (2)	−0.001 (2)	0.0017 (18)	−0.0052 (18)
C3	0.032 (3)	0.017 (2)	0.018 (2)	−0.005 (2)	0.0090 (19)	−0.005 (2)
C4	0.037 (3)	0.013 (2)	0.009 (2)	−0.003 (2)	0.0035 (18)	−0.0017 (18)
C5	0.032 (3)	0.014 (2)	0.018 (2)	0.002 (2)	−0.006 (2)	−0.006 (2)
C6	0.021 (2)	0.013 (2)	0.019 (2)	0.0007 (19)	−0.0012 (18)	−0.0013 (19)
C7	0.010 (2)	0.010 (2)	0.017 (2)	0.0010 (16)	−0.0019 (16)	−0.0065 (18)
N8	0.022 (2)	0.018 (2)	0.0111 (18)	−0.0010 (16)	−0.0003 (15)	−0.0007 (15)
N9	0.022 (2)	0.019 (2)	0.0140 (18)	−0.0021 (17)	0.0018 (15)	−0.0007 (16)
C10	0.021 (2)	0.012 (2)	0.012 (2)	−0.0014 (18)	−0.0026 (17)	−0.0018 (17)
Se11	0.0099 (2)	0.0196 (2)	0.0181 (2)	−0.00013 (18)	−0.00108 (16)	0.00323 (18)
Br12	0.0272 (3)	0.0214 (3)	0.0153 (2)	−0.0024 (2)	−0.00289 (17)	0.00333 (19)
I13	0.0553 (3)	0.0243 (2)	0.01430 (18)	−0.00140 (16)	0.00484 (14)	0.00152 (13)

Geometric parameters (Å, º)

C1—C2	1.398 (7)	C5—H5	0.9500
C1—C6	1.408 (6)	C5—C6	1.388 (6)
C1—C7	1.462 (6)	C6—H6	0.9500
C2—H2	0.9500	C7—N8	1.295 (6)
C2—C3	1.389 (7)	C7—Se11	1.879 (4)
C3—H3	0.9500	N8—N9	1.388 (5)
C3—C4	1.387 (7)	N9—C10	1.284 (6)
C4—C5	1.386 (7)	C10—Se11	1.861 (5)
C4—I13	2.092 (4)	C10—Br12	1.872 (4)
C2—C1—C6	119.6 (4)	C6—C5—H5	119.9
C2—C1—C7	121.0 (4)	C1—C6—H6	120.3

C6—C1—C7	119.4 (4)	C5—C6—C1	119.4 (4)
C1—C2—H2	119.7	C5—C6—H6	120.3
C3—C2—C1	120.5 (5)	C1—C7—Se11	124.0 (3)
C3—C2—H2	119.7	N8—C7—C1	122.0 (4)
C2—C3—H3	120.4	N8—C7—Se11	114.0 (3)
C4—C3—C2	119.2 (5)	C7—N8—N9	115.4 (4)
C4—C3—H3	120.4	C10—N9—N8	112.5 (4)
C3—C4—I13	119.3 (3)	N9—C10—Se11	116.8 (3)
C5—C4—C3	121.1 (4)	N9—C10—Br12	121.2 (3)
C5—C4—I13	119.6 (4)	Se11—C10—Br12	122.0 (2)
C4—C5—H5	119.9	C10—Se11—C7	81.29 (19)
C4—C5—C6	120.2 (4)		

C1—C2—C3—C4	0.4 (7)	C6—C1—C7—Se11	−178.9 (3)
C1—C7—N8—N9	179.4 (4)	C7—C1—C2—C3	179.8 (4)
C1—C7—Se11—C10	−179.4 (4)	C7—C1—C6—C5	180.0 (4)
C2—C1—C6—C5	0.0 (7)	C7—N8—N9—C10	0.3 (6)
C2—C1—C7—N8	−179.5 (4)	N8—C7—Se11—C10	1.1 (3)
C2—C1—C7—Se11	1.1 (6)	N8—N9—C10—Se11	0.7 (5)
C2—C3—C4—C5	−0.4 (7)	N8—N9—C10—Br12	−179.0 (3)
C2—C3—C4—I13	−178.9 (3)	N9—C10—Se11—C7	−1.0 (4)
C3—C4—C5—C6	0.2 (7)	Se11—C7—N8—N9	−1.1 (5)
C4—C5—C6—C1	0.0 (7)	Br12—C10—Se11—C7	178.7 (3)
C6—C1—C2—C3	−0.2 (7)	I13—C4—C5—C6	178.7 (3)
C6—C1—C7—N8	0.6 (6)		

2-Bromo-5-(4-iodophenyl)-1,3,4-thiadiazole (T4)

Crystal data

$C_8H_4BrIN_2S$
M_r = 367.00
Orthorhombic, *Pbca*
a = 10.9919 (2) Å
b = 6.9945 (1) Å
c = 26.4076 (4) Å
V = 2030.29 (6) Å^3
Z = 8
F(000) = 1360

D_x = 2.401 Mg m^{-3}
Cu $K\alpha$ radiation, λ = 1.54184 Å
Cell parameters from 5134 reflections
θ = 3.3–70.6°
μ = 30.95 mm^{-1}
T = 293 K
Plate, colourless
0.05 × 0.04 × 0.01 mm

Data collection

Rigaku XtaLAB Synergy Custom diffractometer with a HyPix-Arc 150° detector
Radiation source: Rotating-anode X-ray tube, Rigaku (Cu) X-ray Source
Mirror monochromator
Detector resolution: 10.0000 pixels mm^{-1}
ω scans
Absorption correction: multi-scan (CrysAlis PRO; Rigaku OD, 2020)

T_{min} = 0.373, T_{max} = 1.000
7258 measured reflections
1920 independent reflections
1802 reflections with $I > 2\sigma(I)$
R_{int} = 0.025
θ_{max} = 70.7°, θ_{min} = 3.4°
h = −13→9
k = −8→7
l = −27→31

Refinement

Refinement on F^2
Least-squares matrix: full
$R[F^2 > 2\sigma(F^2)] = 0.021$
$wR(F^2) = 0.052$
$S = 1.07$
1920 reflections
118 parameters
0 restraints
Primary atom site location: dual
Hydrogen site location: inferred from neighbouring sites
H-atom parameters constrained
$w = 1/[\sigma^2(F_o^2) + (0.0219P)^2 + 2.6464P]$ where $P = (F_o^2 + 2F_c^2)/3$
$(\Delta/\sigma)_{max} = 0.001$
$\Delta\rho_{max} = 0.57$ e Å^{-3}
$\Delta\rho_{min} = -0.67$ e Å^{-3}

Special details

Geometry. All esds (except the esd in the dihedral angle between two l.s. planes) are estimated using the full covariance matrix. The cell esds are taken into account individually in the estimation of esds in distances, angles and torsion angles; correlations between esds in cell parameters are only used when they are defined by crystal symmetry. An approximate (isotropic) treatment of cell esds is used for estimating esds involving l.s. planes.

Fractional atomic coordinates and isotropic or equivalent isotropic displacement parameters (Å²)

	x	*y*	*z*	U_{iso}*/U_{eq}
C1	0.6729 (3)	0.3732 (4)	0.40837 (11)	0.0202 (6)
C2	0.5551 (3)	0.4009 (4)	0.38896 (11)	0.0228 (7)
H2	0.487684	0.378054	0.409375	0.027*
C3	0.5392 (3)	0.4619 (5)	0.33964 (11)	0.0252 (7)
H3	0.461242	0.482985	0.327092	0.030*
C4	0.6391 (3)	0.4915 (5)	0.30907 (11)	0.0245 (7)
C5	0.7571 (3)	0.4651 (5)	0.32710 (11)	0.0232 (6)
H5	0.823891	0.487009	0.306263	0.028*
C6	0.7730 (3)	0.4053 (4)	0.37681 (12)	0.0217 (6)
H6	0.851192	0.386382	0.389268	0.026*
C7	0.6931 (3)	0.3097 (5)	0.46055 (11)	0.0205 (6)
N8	0.8022 (2)	0.2851 (4)	0.47936 (9)	0.0229 (6)
N9	0.8006 (2)	0.2255 (4)	0.52908 (9)	0.0236 (6)
C10	0.6900 (3)	0.2081 (5)	0.54533 (11)	0.0225 (6)
S11	0.57681 (6)	0.25939 (12)	0.50282 (3)	0.02332 (17)
Br12	0.65699 (3)	0.13399 (5)	0.61220 (2)	0.02781 (10)
I13	0.61471 (2)	0.58780 (3)	0.23455 (2)	0.03153 (9)

Atomic displacement parameters (Å²)

	U^{11}	U^{22}	U^{33}	U^{12}	U^{13}	U^{23}
C1	0.0209 (14)	0.0211 (16)	0.0184 (15)	0.0008 (12)	0.0000 (12)	−0.0028 (11)
C2	0.0190 (15)	0.0291 (18)	0.0204 (15)	0.0019 (12)	−0.0010 (12)	−0.0040 (12)
C3	0.0244 (15)	0.0303 (18)	0.0211 (14)	0.0021 (14)	−0.0046 (13)	−0.0044 (13)
C4	0.0322 (16)	0.0261 (17)	0.0152 (14)	0.0011 (14)	−0.0025 (12)	−0.0021 (13)
C5	0.0246 (14)	0.0259 (17)	0.0192 (14)	0.0008 (13)	0.0030 (12)	−0.0013 (13)
C6	0.0202 (14)	0.0236 (16)	0.0214 (15)	−0.0017 (12)	−0.0003 (12)	−0.0004 (12)
C7	0.0158 (13)	0.0244 (16)	0.0214 (14)	0.0011 (13)	0.0022 (11)	−0.0026 (12)
N8	0.0170 (12)	0.0342 (15)	0.0175 (12)	0.0005 (12)	0.0000 (9)	−0.0004 (11)
N9	0.0201 (12)	0.0331 (15)	0.0176 (12)	0.0025 (12)	−0.0008 (10)	−0.0007 (11)

C10	0.0221 (14)	0.0267 (16)	0.0185 (14)	0.0021 (13)	−0.0008 (12)	0.0010 (12)
S11	0.0155 (3)	0.0343 (4)	0.0201 (3)	0.0007 (3)	0.0012 (3)	0.0040 (3)
Br12	0.02913 (18)	0.0356 (2)	0.01864 (17)	0.00341 (15)	0.00365 (13)	0.00393 (13)
I13	0.04468 (15)	0.03386 (14)	0.01605 (12)	0.00057 (10)	−0.00390 (8)	0.00102 (8)

Geometric parameters (Å, º)

C1—C2	1.407 (4)	C5—H5	0.9300
C1—C6	1.398 (4)	C5—C6	1.388 (4)
C1—C7	1.465 (4)	C6—H6	0.9300
C2—H2	0.9300	C7—N8	1.309 (4)
C2—C3	1.382 (4)	C7—S11	1.733 (3)
C3—H3	0.9300	N8—N9	1.378 (3)
C3—C4	1.379 (4)	N9—C10	1.295 (4)
C4—C5	1.394 (4)	C10—S11	1.714 (3)
C4—I13	2.097 (3)	C10—Br12	1.876 (3)
C2—C1—C7	121.6 (3)	C6—C5—H5	120.7
C6—C1—C2	119.0 (3)	C1—C6—H6	119.6
C6—C1—C7	119.4 (3)	C5—C6—C1	120.9 (3)
C1—C2—H2	119.9	C5—C6—H6	119.6
C3—C2—C1	120.2 (3)	C1—C7—S11	123.8 (2)
C3—C2—H2	119.9	N8—C7—C1	122.4 (3)
C2—C3—H3	120.1	N8—C7—S11	113.9 (2)
C4—C3—C2	119.8 (3)	C7—N8—N9	113.0 (2)
C4—C3—H3	120.1	C10—N9—N8	110.8 (2)
C3—C4—C5	121.4 (3)	N9—C10—S11	116.4 (2)
C3—C4—I13	119.7 (2)	N9—C10—Br12	121.3 (2)
C5—C4—I13	118.8 (2)	S11—C10—Br12	122.26 (17)
C4—C5—H5	120.7	C10—S11—C7	85.92 (14)
C6—C5—C4	118.7 (3)		
C1—C2—C3—C4	1.5 (5)	C6—C1—C7—S11	−178.3 (2)
C1—C7—N8—N9	179.9 (3)	C7—C1—C2—C3	179.6 (3)
C1—C7—S11—C10	−179.7 (3)	C7—C1—C6—C5	179.8 (3)
C2—C1—C6—C5	0.5 (5)	C7—N8—N9—C10	0.0 (4)
C2—C1—C7—N8	−179.3 (3)	N8—C7—S11—C10	0.6 (3)
C2—C1—C7—S11	1.0 (4)	N8—N9—C10—S11	0.5 (4)
C2—C3—C4—C5	−1.4 (5)	N8—N9—C10—Br12	−178.7 (2)
C2—C3—C4—I13	−179.2 (2)	N9—C10—S11—C7	−0.6 (3)
C3—C4—C5—C6	0.8 (5)	S11—C7—N8—N9	−0.5 (4)
C4—C5—C6—C1	−0.4 (5)	Br12—C10—S11—C7	178.6 (2)
C6—C1—C2—C3	−1.0 (5)	I13—C4—C5—C6	178.6 (2)
C6—C1—C7—N8	1.3 (5)		

supporting information

Acta Cryst. (2022). C**78**, 716-721 [https://doi.org/10.1107/S205322962201052X]

Competition between chalcogen and halogen bonding assessed through isostructural species

Viraj De Silva, Pierre Le Magueres, Boris B. Averkiev and Christer B. Aakeröy

Computing details

Data collection: *CrysAlis PRO* (Rigaku OD, 2020) for T1, T4; *CrysAlis PRO* 1.171.41.76a (Rigaku OD, 2020) for T2; *CrysAlis PRO* 1.171.40.84a (Rigaku OD, 2020) for T3. Cell refinement: *CrysAlis PRO* (Rigaku OD, 2020) for T1, T4; *CrysAlis PRO* 1.171.41.76a (Rigaku OD, 2020) for T2; *CrysAlis PRO* 1.171.40.84a (Rigaku OD, 2020) for T3. Data reduction: *CrysAlis PRO* (Rigaku OD, 2020) for T1, T4; *CrysAlis PRO* 1.171.41.76a (Rigaku OD, 2020) for T2; *CrysAlis PRO* 1.171.40.84a (Rigaku OD, 2020) for T3. Program(s) used to solve structure: SHELXT2018 (Sheldrick, 2015*a*) for T1; SHELXT (Sheldrick, 2015*a*) for T2, T3, T4. For all structures, program(s) used to refine structure: *SHELXL2018* (Sheldrick, 2015*b*); molecular graphics: OLEX2 (Dolomanov *et al.*, 2009); software used to prepare material for publication: OLEX2 (Dolomanov *et al.*, 2009).

2-Iodo-5-(4-iodophenyl)-1,3,4-thiadiazole (T1)

Crystal data

$C_8H_4I_2N_2S$
M_r = 413.99
Orthorhombic, *Pbca*
a = 11.0392 (2) Å
b = 8.1756 (2) Å
c = 23.3673 (4) Å
V = 2108.95 (7) Å^3
Z = 8
F(000) = 1504
D_x = 2.608 Mg m^{-3}
Cu *Kα* radiation, *λ* = 1.54184 Å
Cell parameters from 5508 reflections
θ = 3.8–69.0°
μ = 48.34 mm^{-1}
T = 293 K
Block, colourless
0.07 × 0.05 × 0.03 mm

Data collection

Rigaku XtaLAB Synergy Custom diffractometer with a HyPix-Arc 150° detector
Radiation source: Rotating-anode X-ray tube, Rigaku (Cu) X-ray Source
Mirror monochromator
Detector resolution: 10.0000 pixels mm^{-1}
ω scans
Absorption correction: gaussian (CrysAlis PRO; Rigaku OD, 2020)
T_{min} = 0.209, T_{max} = 0.522
8336 measured reflections
1942 independent reflections
1753 reflections with $I > 2\sigma(I)$
R_{int} = 0.024
θ_{max} = 69.1°, θ_{min} = 3.8°
h = −11→13
k = −8→9
l = −24→28

Refinement

Refinement on F^2
Least-squares matrix: full
$R[F^2 > 2\sigma(F^2)]$ = 0.026
$wR(F^2)$ = 0.071
S = 1.09
1942 reflections
118 parameters
0 restraints

Primary atom site location: dual
Hydrogen site location: inferred from neighbouring sites
H-atom parameters constrained

$w = 1/[\sigma^2(F_o^2) + (0.0388P)^2 + 4.6153P]$ where $P = (F_o^2 + 2F_c^2)/3$
$(\Delta/\sigma)_{max} = 0.001$
$\Delta\rho_{max} = 1.33$ e Å^{-3}
$\Delta\rho_{min} = -1.22$ e Å^{-3}

Special details

Geometry. All esds (except the esd in the dihedral angle between two l.s. planes) are estimated using the full covariance matrix. The cell esds are taken into account individually in the estimation of esds in distances, angles and torsion angles; correlations between esds in cell parameters are only used when they are defined by crystal symmetry. An approximate (isotropic) treatment of cell esds is used for estimating esds involving l.s. planes.

Fractional atomic coordinates and isotropic or equivalent isotropic displacement parameters (Å²)

	x	*y*	*z*	U_{iso}*/U_{eq}
C1	0.6455 (4)	0.4015 (5)	0.40675 (18)	0.0196 (9)
C2	0.5284 (4)	0.4540 (6)	0.39544 (19)	0.0209 (9)
H2	0.465059	0.421230	0.419049	0.025*
C3	0.5054 (4)	0.5556 (5)	0.34887 (18)	0.0207 (9)
H3	0.427089	0.591795	0.341467	0.025*
C4	0.6006 (4)	0.6024 (5)	0.31353 (18)	0.0218 (9)
C5	0.7186 (4)	0.5514 (5)	0.32447 (19)	0.0245 (10)
H5	0.782009	0.584936	0.301019	0.029*
C6	0.7402 (4)	0.4498 (6)	0.37097 (18)	0.0219 (9)
H6	0.818500	0.413535	0.378344	0.026*
C7	0.6712 (4)	0.2974 (5)	0.45654 (18)	0.0205 (9)
N8	0.7801 (3)	0.2525 (4)	0.47101 (17)	0.0242 (9)
N9	0.7827 (3)	0.1583 (5)	0.52011 (16)	0.0243 (8)
C10	0.6745 (4)	0.1372 (5)	0.54045 (18)	0.0212 (9)
S11	0.55940 (10)	0.22850 (15)	0.50283 (5)	0.0246 (3)
I12	0.64084 (3)	0.00912 (3)	0.61590 (2)	0.02546 (12)
I13	0.56375 (3)	0.75148 (3)	0.24272 (2)	0.02576 (12)

Atomic displacement parameters (Å²)

	U^{11}	U^{22}	U^{33}	U^{12}	U^{13}	U^{23}
C1	0.021 (2)	0.018 (2)	0.020 (2)	0.0000 (17)	0.0006 (17)	−0.0003 (18)
C2	0.019 (2)	0.020 (2)	0.023 (2)	−0.0004 (18)	0.0016 (18)	−0.0021 (18)
C3	0.021 (2)	0.020 (2)	0.021 (2)	0.0020 (18)	0.0001 (18)	0.0002 (18)
C4	0.028 (2)	0.0163 (19)	0.021 (2)	0.0016 (18)	0.0005 (19)	−0.0001 (17)
C5	0.027 (2)	0.019 (2)	0.027 (2)	−0.0020 (19)	0.0067 (18)	−0.0058 (19)
C6	0.021 (2)	0.017 (2)	0.028 (2)	−0.0010 (18)	0.0026 (19)	−0.0052 (18)
C7	0.022 (2)	0.019 (2)	0.020 (2)	−0.0014 (18)	−0.0009 (18)	0.0002 (18)
N8	0.021 (2)	0.027 (2)	0.0241 (19)	0.0015 (16)	−0.0022 (15)	0.0023 (16)
N9	0.024 (2)	0.027 (2)	0.0223 (17)	0.0037 (17)	−0.0021 (16)	0.0015 (16)
C10	0.022 (2)	0.018 (2)	0.024 (2)	0.0003 (18)	−0.0040 (19)	−0.0023 (18)
S11	0.0187 (6)	0.0283 (6)	0.0267 (6)	0.0013 (4)	−0.0004 (4)	0.0053 (5)
I12	0.0279 (2)	0.02557 (18)	0.02293 (18)	0.00177 (11)	−0.00234 (11)	0.00194 (11)
I13	0.0349 (2)	0.02059 (18)	0.02173 (18)	−0.00176 (11)	−0.00195 (11)	0.00162 (11)

Geometric parameters (Å, º)

C1—C2	1.388 (6)	C5—H5	0.9300
C1—C6	1.395 (6)	C5—C6	1.389 (6)
C1—C7	1.469 (6)	C6—H6	0.9300
C2—H2	0.9300	C7—N8	1.302 (6)
C2—C3	1.392 (6)	C7—S11	1.735 (4)
C3—H3	0.9300	N8—N9	1.382 (5)
C3—C4	1.390 (6)	N9—C10	1.297 (6)
C4—C5	1.391 (6)	C10—S11	1.716 (4)
C4—I13	2.095 (4)	C10—I12	2.084 (4)
C2—C1—C6	119.7 (4)	C6—C5—H5	120.5
C2—C1—C7	120.6 (4)	C1—C6—H6	119.7
C6—C1—C7	119.6 (4)	C5—C6—C1	120.7 (4)
C1—C2—H2	119.9	C5—C6—H6	119.7
C1—C2—C3	120.2 (4)	C1—C7—S11	123.0 (3)
C3—C2—H2	119.9	N8—C7—C1	123.2 (4)
C2—C3—H3	120.3	N8—C7—S11	113.8 (3)
C4—C3—C2	119.4 (4)	C7—N8—N9	113.1 (4)
C4—C3—H3	120.3	C10—N9—N8	111.1 (3)
C3—C4—C5	121.1 (4)	N9—C10—S11	115.9 (3)
C3—C4—I13	118.8 (3)	N9—C10—I12	122.8 (3)
C5—C4—I13	120.1 (3)	S11—C10—I12	121.3 (2)
C4—C5—H5	120.5	C10—S11—C7	86.2 (2)
C6—C5—C4	118.9 (4)		
C1—C2—C3—C4	0.7 (7)	C6—C1—C7—S11	−179.0 (3)
C1—C7—N8—N9	178.4 (4)	C7—C1—C2—C3	178.6 (4)
C1—C7—S11—C10	−178.5 (4)	C7—C1—C6—C5	−178.4 (4)
C2—C1—C6—C5	0.7 (7)	C7—N8—N9—C10	−0.1 (5)
C2—C1—C7—N8	−175.9 (4)	N8—C7—S11—C10	−0.4 (4)
C2—C1—C7—S11	1.9 (6)	N8—N9—C10—S11	−0.2 (5)
C2—C3—C4—C5	−1.0 (6)	N8—N9—C10—I12	−177.7 (3)
C2—C3—C4—I13	178.8 (3)	N9—C10—S11—C7	0.3 (4)
C3—C4—C5—C6	1.2 (6)	S11—C7—N8—N9	0.4 (5)
C4—C5—C6—C1	−1.0 (7)	I12—C10—S11—C7	177.9 (3)
C6—C1—C2—C3	−0.5 (7)	I13—C4—C5—C6	−178.6 (3)
C6—C1—C7—N8	3.2 (7)		

2-Bromo-5-(4-bromophenyl)-1,3,4-selenadiazole (T2)

Crystal data

$C_8H_4Br_2N_2Se$
M_r = 366.91
Orthorhombic, *Pbca*
a = 11.1945 (5) Å
b = 7.1006 (3) Å
c = 25.4725 (9) Å
V = 2024.74 (15) Å^3
Z = 8
F(000) = 1360
D_x = 2.407 Mg m^{-3}
Cu *Kα* radiation, *λ* = 1.54184 Å
Cell parameters from 3007 reflections
θ = 3.5–74.7°
μ = 13.90 mm^{-1}

T = 100 K
Irregular, orange

0.02 × 0.02 × 0.02 mm

Data collection

Rigaku XtaLAB Synergy Custom diffractometer with a HyPix-Arc 150° detector
Radiation source: micro-focus sealed X-ray tube, PhotonJet (Cu) X-ray Source
Mirror monochromator
Detector resolution: 10.0000 pixels mm^{-1}
ω scans
Absorption correction: multi-scan (CrysAlis PRO; Rigaku OD, 2020)

T_{min} = 0.682, T_{max} = 1.000
6457 measured reflections
1965 independent reflections
1709 reflections with $I > 2\sigma(I)$
R_{int} = 0.037
θ_{max} = 74.8°, θ_{min} = 3.5°
h = −9→13
k = −8→8
l = −29→30

Refinement

Refinement on F^2
Least-squares matrix: full
$R[F^2 > 2\sigma(F^2)]$ = 0.044
$wR(F^2)$ = 0.109
S = 1.05
1965 reflections
118 parameters
0 restraints
Primary atom site location: dual

Hydrogen site location: inferred from neighbouring sites
H-atom parameters constrained
$w = 1/[\sigma^2(F_o^2) + (0.0428P)^2 + 15.9376P]$ where $P = (F_o^2 + 2F_c^2)/3$
$(\Delta/\sigma)_{max}$ = 0.001
$\Delta\rho_{max}$ = 1.95 e Å^{-3}
$\Delta\rho_{min}$ = −1.46 e Å^{-3}

Special details

Geometry. All esds (except the esd in the dihedral angle between two l.s. planes) are estimated using the full covariance matrix. The cell esds are taken into account individually in the estimation of esds in distances, angles and torsion angles; correlations between esds in cell parameters are only used when they are defined by crystal symmetry. An approximate (isotropic) treatment of cell esds is used for estimating esds involving l.s. planes.

Fractional atomic coordinates and isotropic or equivalent isotropic displacement parameters (Å^2)

	x	y	z	U_{iso}*/U_{eq}
C1	0.3302 (5)	0.3834 (8)	0.5943 (2)	0.0221 (12)
C2	0.4462 (6)	0.4100 (9)	0.6138 (2)	0.0281 (13)
H2	0.513177	0.382973	0.592141	0.034*
C3	0.4634 (7)	0.4753 (9)	0.6643 (3)	0.0350 (15)
H3	0.541775	0.495041	0.677551	0.042*
C4	0.3654 (7)	0.5113 (9)	0.6952 (2)	0.0329 (15)
C5	0.2498 (7)	0.4874 (8)	0.6768 (2)	0.0316 (14)
H5	0.183353	0.515334	0.698698	0.038*
C6	0.2326 (6)	0.4222 (8)	0.6263 (2)	0.0276 (13)
H6	0.153883	0.403931	0.613314	0.033*
C7	0.3101 (5)	0.3151 (8)	0.5401 (2)	0.0180 (11)
N8	0.2045 (4)	0.2908 (7)	0.52118 (18)	0.0227 (10)
N9	0.2012 (4)	0.2252 (7)	0.46988 (18)	0.0227 (10)
C10	0.3064 (5)	0.2028 (8)	0.4508 (2)	0.0211 (12)
Se11	0.43492 (5)	0.25540 (9)	0.49395 (2)	0.02259 (19)
Br12	0.32759 (6)	0.11997 (9)	0.38120 (2)	0.0301 (2)
Br13	0.39006 (10)	0.60799 (12)	0.76394 (3)	0.0541 (3)

Atomic displacement parameters (Å²)

	U^{11}	U^{22}	U^{33}	U^{12}	U^{13}	U^{23}
C1	0.033 (3)	0.017 (3)	0.016 (3)	0.000 (2)	−0.001 (2)	0.002 (2)
C2	0.036 (3)	0.030 (3)	0.018 (3)	−0.008 (3)	−0.002 (3)	0.009 (2)
C3	0.048 (4)	0.031 (3)	0.026 (3)	−0.007 (3)	−0.010 (3)	0.007 (3)
C4	0.059 (4)	0.026 (3)	0.014 (3)	−0.003 (3)	−0.002 (3)	0.004 (2)
C5	0.053 (4)	0.018 (3)	0.023 (3)	0.005 (3)	0.008 (3)	0.002 (3)
C6	0.034 (3)	0.020 (3)	0.028 (3)	0.004 (3)	0.000 (3)	0.002 (2)
C7	0.017 (3)	0.013 (2)	0.024 (3)	0.002 (2)	−0.001 (2)	0.002 (2)
N8	0.023 (2)	0.027 (3)	0.018 (2)	−0.002 (2)	0.0004 (19)	0.005 (2)
N9	0.024 (2)	0.024 (3)	0.020 (2)	−0.003 (2)	−0.0022 (19)	0.002 (2)
C10	0.026 (3)	0.017 (3)	0.020 (3)	−0.003 (2)	0.002 (2)	0.001 (2)
Se11	0.0167 (3)	0.0242 (3)	0.0269 (3)	−0.0007 (2)	0.0013 (2)	−0.0020 (2)
Br12	0.0405 (4)	0.0285 (3)	0.0213 (3)	−0.0041 (3)	0.0050 (3)	−0.0039 (3)
Br13	0.1013 (8)	0.0407 (4)	0.0205 (3)	−0.0056 (5)	−0.0081 (4)	−0.0012 (3)

Geometric parameters (Å, º)

C1—C2	1.403 (9)	C5—H5	0.9500
C1—C6	1.391 (9)	C5—C6	1.382 (8)
C1—C7	1.479 (8)	C6—H6	0.9500
C2—H2	0.9500	C7—N8	1.288 (7)
C2—C3	1.383 (9)	C7—Se11	1.876 (5)
C3—H3	0.9500	N8—N9	1.388 (7)
C3—C4	1.373 (10)	N9—C10	1.284 (7)
C4—C5	1.387 (10)	C10—Se11	1.849 (6)
C4—Br13	1.901 (6)	C10—Br12	1.882 (6)
C2—C1—C7	121.0 (5)	C6—C5—H5	120.5
C6—C1—C2	119.5 (5)	C1—C6—H6	119.9
C6—C1—C7	119.4 (5)	C5—C6—C1	120.2 (6)
C1—C2—H2	119.9	C5—C6—H6	119.9
C3—C2—C1	120.3 (6)	C1—C7—Se11	123.0 (4)
C3—C2—H2	119.9	N8—C7—C1	122.2 (5)
C2—C3—H3	120.5	N8—C7—Se11	114.7 (4)
C4—C3—C2	119.0 (6)	C7—N8—N9	115.0 (5)
C4—C3—H3	120.5	C10—N9—N8	112.0 (5)
C3—C4—C5	122.0 (6)	N9—C10—Se11	117.6 (4)
C3—C4—Br13	118.6 (5)	N9—C10—Br12	120.7 (4)
C5—C4—Br13	119.3 (5)	Se11—C10—Br12	121.7 (3)
C4—C5—H5	120.5	C10—Se11—C7	80.7 (2)
C6—C5—C4	119.0 (6)		
C1—C2—C3—C4	0.8 (9)	C6—C1—C7—Se11	−179.2 (4)
C1—C7—N8—N9	−179.7 (5)	C7—C1—C2—C3	179.5 (5)
C1—C7—Se11—C10	−179.8 (5)	C7—C1—C6—C5	−179.6 (5)
C2—C1—C6—C5	0.3 (9)	C7—N8—N9—C10	−0.6 (7)

C2—C1—C7—N8	−179.5 (5)	N8—C7—Se11—C10	0.6 (4)
C2—C1—C7—Se11	1.0 (8)	N8—N9—C10—Se11	1.1 (6)
C2—C3—C4—C5	−1.2 (10)	N8—N9—C10—Br12	−178.7 (4)
C2—C3—C4—Br13	−178.2 (5)	N9—C10—Se11—C7	−1.0 (5)
C3—C4—C5—C6	1.2 (9)	Se11—C7—N8—N9	−0.2 (6)
C4—C5—C6—C1	−0.7 (9)	Br12—C10—Se11—C7	178.8 (4)
C6—C1—C2—C3	−0.3 (9)	Br13—C4—C5—C6	178.1 (4)
C6—C1—C7—N8	0.3 (8)		

2-Bromo-5-(4-iodophenyl)-1,3,4-selenadiazole (T3)

Crystal data

$C_8H_4BrIN_2Se$
$M_r = 413.90$
Orthorhombic, *Pbca*
$a = 11.1735$ (4) Å
$b = 7.1222$ (2) Å
$c = 26.1875$ (8) Å
$V = 2084.00$ (11) Å^3
$Z = 8$
$F(000) = 1504$
$D_x = 2.638$ Mg m^{-3}
Mo $K\alpha$ radiation, $\lambda = 0.71073$ Å
Cell parameters from 7358 reflections
$\theta = 2.4$–$33.0°$
$\mu = 10.36$ mm^{-1}
$T = 100$ K
Plate, clear light yellow
0.3 × 0.1 × 0.06 mm

Data collection

Rigaku XtaLAB Synergy Custom diffractometer with a HyPix-Arc 150° detector
Radiation source: micro-focus sealed X-ray tube, PhotonJet (Mo) X-ray Source
Mirror monochromator
Detector resolution: 10.0000 pixels mm^{-1}
ω scans
Absorption correction: multi-scan (CrysAlis PRO; Rigaku OD, 2020)
$T_{min} = 0.338$, $T_{max} = 1.000$
12091 measured reflections
2055 independent reflections
1815 reflections with $I > 2\sigma(I)$
$R_{int} = 0.035$
$\theta_{max} = 26.0°$, $\theta_{min} = 2.4°$
$h = -13 \rightarrow 13$
$k = -7 \rightarrow 8$
$l = -32 \rightarrow 32$

Refinement

Refinement on F^2
Least-squares matrix: full
$R[F^2 > 2\sigma(F^2)] = 0.030$
$wR(F^2) = 0.070$
$S = 1.08$
2055 reflections
118 parameters
0 restraints
Primary atom site location: dual
Hydrogen site location: inferred from neighbouring sites
H-atom parameters constrained
$w = 1/[\sigma^2(F_o^2) + (0.030P)^2 + 10.0022P]$ where $P = (F_o^2 + 2F_c^2)/3$
$(\Delta/\sigma)_{max} = 0.001$
$\Delta\rho_{max} = 2.00$ e Å^{-3}
$\Delta\rho_{min} = -1.01$ e Å^{-3}

Special details

Geometry. All esds (except the esd in the dihedral angle between two l.s. planes) are estimated using the full covariance matrix. The cell esds are taken into account individually in the estimation of esds in distances, angles and torsion angles; correlations between esds in cell parameters are only used when they are defined by crystal symmetry. An approximate (isotropic) treatment of cell esds is used for estimating esds involving l.s. planes.

Fractional atomic coordinates and isotropic or equivalent isotropic displacement parameters (Å^2)

	x	*y*	*z*	U_{iso}*/U_{eq}
C1	0.6730 (4)	0.6139 (6)	0.59069 (17)	0.0149 (9)

C2	0.5578 (4)	0.5876 (7)	0.61022 (17)	0.0196 (10)
H2	0.4902	0.6141	0.5894	0.023*
C3	0.5414 (5)	0.5230 (7)	0.65978 (18)	0.0226 (10)
H3	0.4630	0.5045	0.6729	0.027*
C4	0.6408 (5)	0.4859 (6)	0.68987 (16)	0.0195 (10)
C5	0.7557 (5)	0.5112 (6)	0.67115 (17)	0.0213 (10)
H5	0.8227	0.4847	0.6923	0.026*
C6	0.7731 (4)	0.5751 (6)	0.62163 (17)	0.0176 (10)
H6	0.8518	0.5925	0.6087	0.021*
C7	0.6914 (4)	0.6814 (6)	0.53853 (16)	0.0122 (9)
N8	0.7974 (3)	0.7053 (5)	0.51957 (14)	0.0171 (8)
N9	0.8006 (3)	0.7683 (5)	0.46942 (14)	0.0184 (8)
C10	0.6957 (4)	0.7927 (6)	0.45060 (17)	0.0151 (9)
Se11	0.56664 (4)	0.74266 (7)	0.49341 (2)	0.01587 (12)
Br12	0.67471 (4)	0.87353 (7)	0.38316 (2)	0.02129 (13)
I13	0.61637 (4)	0.38409 (5)	0.76407 (2)	0.03129 (12)

Atomic displacement parameters (Å²)

	U^{11}	U^{22}	U^{33}	U^{12}	U^{13}	U^{23}
C1	0.021 (2)	0.009 (2)	0.015 (2)	0.0004 (18)	0.0006 (17)	−0.0032 (17)
C2	0.024 (2)	0.020 (2)	0.015 (2)	−0.001 (2)	0.0017 (18)	−0.0052 (18)
C3	0.032 (3)	0.017 (2)	0.018 (2)	−0.005 (2)	0.0090 (19)	−0.005 (2)
C4	0.037 (3)	0.013 (2)	0.009 (2)	−0.003 (2)	0.0035 (18)	−0.0017 (18)
C5	0.032 (3)	0.014 (2)	0.018 (2)	0.002 (2)	−0.006 (2)	−0.006 (2)
C6	0.021 (2)	0.013 (2)	0.019 (2)	0.0007 (19)	−0.0012 (18)	−0.0013 (19)
C7	0.010 (2)	0.010 (2)	0.017 (2)	0.0010 (16)	−0.0019 (16)	−0.0065 (18)
N8	0.022 (2)	0.018 (2)	0.0111 (18)	−0.0010 (16)	−0.0003 (15)	−0.0007 (15)
N9	0.022 (2)	0.019 (2)	0.0140 (18)	−0.0021 (17)	0.0018 (15)	−0.0007 (16)
C10	0.021 (2)	0.012 (2)	0.012 (2)	−0.0014 (18)	−0.0026 (17)	−0.0018 (17)
Se11	0.0099 (2)	0.0196 (2)	0.0181 (2)	−0.00013 (18)	−0.00108 (16)	0.00323 (18)
Br12	0.0272 (3)	0.0214 (3)	0.0153 (2)	−0.0024 (2)	−0.00289 (17)	0.00333 (19)
I13	0.0553 (3)	0.0243 (2)	0.01430 (18)	−0.00140 (16)	0.00484 (14)	0.00152 (13)

Geometric parameters (Å, º)

C1—C2	1.398 (7)	C5—H5	0.9500
C1—C6	1.408 (6)	C5—C6	1.388 (6)
C1—C7	1.462 (6)	C6—H6	0.9500
C2—H2	0.9500	C7—N8	1.295 (6)
C2—C3	1.389 (7)	C7—Se11	1.879 (4)
C3—H3	0.9500	N8—N9	1.388 (5)
C3—C4	1.387 (7)	N9—C10	1.284 (6)
C4—C5	1.386 (7)	C10—Se11	1.861 (5)
C4—I13	2.092 (4)	C10—Br12	1.872 (4)
C2—C1—C6	119.6 (4)	C6—C5—H5	119.9
C2—C1—C7	121.0 (4)	C1—C6—H6	120.3

C6—C1—C7	119.4 (4)	C5—C6—C1	119.4 (4)
C1—C2—H2	119.7	C5—C6—H6	120.3
C3—C2—C1	120.5 (5)	C1—C7—Se11	124.0 (3)
C3—C2—H2	119.7	N8—C7—C1	122.0 (4)
C2—C3—H3	120.4	N8—C7—Se11	114.0 (3)
C4—C3—C2	119.2 (5)	C7—N8—N9	115.4 (4)
C4—C3—H3	120.4	C10—N9—N8	112.5 (4)
C3—C4—I13	119.3 (3)	N9—C10—Se11	116.8 (3)
C5—C4—C3	121.1 (4)	N9—C10—Br12	121.2 (3)
C5—C4—I13	119.6 (4)	Se11—C10—Br12	122.0 (2)
C4—C5—H5	119.9	C10—Se11—C7	81.29 (19)
C4—C5—C6	120.2 (4)		

C1—C2—C3—C4	0.4 (7)	C6—C1—C7—Se11	−178.9 (3)
C1—C7—N8—N9	179.4 (4)	C7—C1—C2—C3	179.8 (4)
C1—C7—Se11—C10	−179.4 (4)	C7—C1—C6—C5	180.0 (4)
C2—C1—C6—C5	0.0 (7)	C7—N8—N9—C10	0.3 (6)
C2—C1—C7—N8	−179.5 (4)	N8—C7—Se11—C10	1.1 (3)
C2—C1—C7—Se11	1.1 (6)	N8—N9—C10—Se11	0.7 (5)
C2—C3—C4—C5	−0.4 (7)	N8—N9—C10—Br12	−179.0 (3)
C2—C3—C4—I13	−178.9 (3)	N9—C10—Se11—C7	−1.0 (4)
C3—C4—C5—C6	0.2 (7)	Se11—C7—N8—N9	−1.1 (5)
C4—C5—C6—C1	0.0 (7)	Br12—C10—Se11—C7	178.7 (3)
C6—C1—C2—C3	−0.2 (7)	I13—C4—C5—C6	178.7 (3)
C6—C1—C7—N8	0.6 (6)		

2-Bromo-5-(4-iodophenyl)-1,3,4-thiadiazole (T4)

Crystal data

$C_8H_4BrIN_2S$
M_r = 367.00
Orthorhombic, *Pbca*
a = 10.9919 (2) Å
b = 6.9945 (1) Å
c = 26.4076 (4) Å
V = 2030.29 (6) Å^3
Z = 8
F(000) = 1360

D_x = 2.401 Mg m^{-3}
Cu $K\alpha$ radiation, λ = 1.54184 Å
Cell parameters from 5134 reflections
θ = 3.3–70.6°
μ = 30.95 mm^{-1}
T = 293 K
Plate, colourless
0.05 × 0.04 × 0.01 mm

Data collection

Rigaku XtaLAB Synergy Custom diffractometer with a HyPix-Arc 150° detector
Radiation source: Rotating-anode X-ray tube, Rigaku (Cu) X-ray Source
Mirror monochromator
Detector resolution: 10.0000 pixels mm^{-1}
ω scans
Absorption correction: multi-scan (CrysAlis PRO; Rigaku OD, 2020)

T_{min} = 0.373, T_{max} = 1.000
7258 measured reflections
1920 independent reflections
1802 reflections with $I > 2\sigma(I)$
R_{int} = 0.025
θ_{max} = 70.7°, θ_{min} = 3.4°
h = −13→9
k = −8→7
l = −27→31

Refinement

Refinement on F^2
Least-squares matrix: full
$R[F^2 > 2\sigma(F^2)] = 0.021$
$wR(F^2) = 0.052$
$S = 1.07$
1920 reflections
118 parameters
0 restraints
Primary atom site location: dual
Hydrogen site location: inferred from neighbouring sites
H-atom parameters constrained
$w = 1/[\sigma^2(F_o^2) + (0.0219P)^2 + 2.6464P]$ where $P = (F_o^2 + 2F_c^2)/3$
$(\Delta/\sigma)_{max} = 0.001$
$\Delta\rho_{max} = 0.57$ e Å^{-3}
$\Delta\rho_{min} = -0.67$ e Å^{-3}

Special details

Geometry. All esds (except the esd in the dihedral angle between two l.s. planes) are estimated using the full covariance matrix. The cell esds are taken into account individually in the estimation of esds in distances, angles and torsion angles; correlations between esds in cell parameters are only used when they are defined by crystal symmetry. An approximate (isotropic) treatment of cell esds is used for estimating esds involving l.s. planes.

Fractional atomic coordinates and isotropic or equivalent isotropic displacement parameters (Å²)

	x	*y*	*z*	U_{iso}*/U_{eq}
C1	0.6729 (3)	0.3732 (4)	0.40837 (11)	0.0202 (6)
C2	0.5551 (3)	0.4009 (4)	0.38896 (11)	0.0228 (7)
H2	0.487684	0.378054	0.409375	0.027*
C3	0.5392 (3)	0.4619 (5)	0.33964 (11)	0.0252 (7)
H3	0.461242	0.482985	0.327092	0.030*
C4	0.6391 (3)	0.4915 (5)	0.30907 (11)	0.0245 (7)
C5	0.7571 (3)	0.4651 (5)	0.32710 (11)	0.0232 (6)
H5	0.823891	0.487009	0.306263	0.028*
C6	0.7730 (3)	0.4053 (4)	0.37681 (12)	0.0217 (6)
H6	0.851192	0.386382	0.389268	0.026*
C7	0.6931 (3)	0.3097 (5)	0.46055 (11)	0.0205 (6)
N8	0.8022 (2)	0.2851 (4)	0.47936 (9)	0.0229 (6)
N9	0.8006 (2)	0.2255 (4)	0.52908 (9)	0.0236 (6)
C10	0.6900 (3)	0.2081 (5)	0.54533 (11)	0.0225 (6)
S11	0.57681 (6)	0.25939 (12)	0.50282 (3)	0.02332 (17)
Br12	0.65699 (3)	0.13399 (5)	0.61220 (2)	0.02781 (10)
I13	0.61471 (2)	0.58780 (3)	0.23455 (2)	0.03153 (9)

Atomic displacement parameters (Å²)

	U^{11}	U^{22}	U^{33}	U^{12}	U^{13}	U^{23}
C1	0.0209 (14)	0.0211 (16)	0.0184 (15)	0.0008 (12)	0.0000 (12)	−0.0028 (11)
C2	0.0190 (15)	0.0291 (18)	0.0204 (15)	0.0019 (12)	−0.0010 (12)	−0.0040 (12)
C3	0.0244 (15)	0.0303 (18)	0.0211 (14)	0.0021 (14)	−0.0046 (13)	−0.0044 (13)
C4	0.0322 (16)	0.0261 (17)	0.0152 (14)	0.0011 (14)	−0.0025 (12)	−0.0021 (13)
C5	0.0246 (14)	0.0259 (17)	0.0192 (14)	0.0008 (13)	0.0030 (12)	−0.0013 (13)
C6	0.0202 (14)	0.0236 (16)	0.0214 (15)	−0.0017 (12)	−0.0003 (12)	−0.0004 (12)
C7	0.0158 (13)	0.0244 (16)	0.0214 (14)	0.0011 (13)	0.0022 (11)	−0.0026 (12)
N8	0.0170 (12)	0.0342 (15)	0.0175 (12)	0.0005 (12)	0.0000 (9)	−0.0004 (11)
N9	0.0201 (12)	0.0331 (15)	0.0176 (12)	0.0025 (12)	−0.0008 (10)	−0.0007 (11)

C10	0.0221 (14)	0.0267 (16)	0.0185 (14)	0.0021 (13)	−0.0008 (12)	0.0010 (12)
S11	0.0155 (3)	0.0343 (4)	0.0201 (3)	0.0007 (3)	0.0012 (3)	0.0040 (3)
Br12	0.02913 (18)	0.0356 (2)	0.01864 (17)	0.00341 (15)	0.00365 (13)	0.00393 (13)
I13	0.04468 (15)	0.03386 (14)	0.01605 (12)	0.00057 (10)	−0.00390 (8)	0.00102 (8)

Geometric parameters (Å, º)

C1—C2	1.407 (4)	C5—H5	0.9300
C1—C6	1.398 (4)	C5—C6	1.388 (4)
C1—C7	1.465 (4)	C6—H6	0.9300
C2—H2	0.9300	C7—N8	1.309 (4)
C2—C3	1.382 (4)	C7—S11	1.733 (3)
C3—H3	0.9300	N8—N9	1.378 (3)
C3—C4	1.379 (4)	N9—C10	1.295 (4)
C4—C5	1.394 (4)	C10—S11	1.714 (3)
C4—I13	2.097 (3)	C10—Br12	1.876 (3)
C2—C1—C7	121.6 (3)	C6—C5—H5	120.7
C6—C1—C2	119.0 (3)	C1—C6—H6	119.6
C6—C1—C7	119.4 (3)	C5—C6—C1	120.9 (3)
C1—C2—H2	119.9	C5—C6—H6	119.6
C3—C2—C1	120.2 (3)	C1—C7—S11	123.8 (2)
C3—C2—H2	119.9	N8—C7—C1	122.4 (3)
C2—C3—H3	120.1	N8—C7—S11	113.9 (2)
C4—C3—C2	119.8 (3)	C7—N8—N9	113.0 (2)
C4—C3—H3	120.1	C10—N9—N8	110.8 (2)
C3—C4—C5	121.4 (3)	N9—C10—S11	116.4 (2)
C3—C4—I13	119.7 (2)	N9—C10—Br12	121.3 (2)
C5—C4—I13	118.8 (2)	S11—C10—Br12	122.26 (17)
C4—C5—H5	120.7	C10—S11—C7	85.92 (14)
C6—C5—C4	118.7 (3)		
C1—C2—C3—C4	1.5 (5)	C6—C1—C7—S11	−178.3 (2)
C1—C7—N8—N9	179.9 (3)	C7—C1—C2—C3	179.6 (3)
C1—C7—S11—C10	−179.7 (3)	C7—C1—C6—C5	179.8 (3)
C2—C1—C6—C5	0.5 (5)	C7—N8—N9—C10	0.0 (4)
C2—C1—C7—N8	−179.3 (3)	N8—C7—S11—C10	0.6 (3)
C2—C1—C7—S11	1.0 (4)	N8—N9—C10—S11	0.5 (4)
C2—C3—C4—C5	−1.4 (5)	N8—N9—C10—Br12	−178.7 (2)
C2—C3—C4—I13	−179.2 (2)	N9—C10—S11—C7	−0.6 (3)
C3—C4—C5—C6	0.8 (5)	S11—C7—N8—N9	−0.5 (4)
C4—C5—C6—C1	−0.4 (5)	Br12—C10—S11—C7	178.6 (2)
C6—C1—C2—C3	−1.0 (5)	I13—C4—C5—C6	178.6 (2)
C6—C1—C7—N8	1.3 (5)		